h_da
HOCHSCHULE DARMSTADT
UNIVERSITY OF APPLIED SCIENCES

Hochschule Darmstadt
- Fachbereich Informatik -

Influence of Image Compression on Ear Biometrics

Abschlussarbeit zur Erlangung des akademischen Grades
Bachelor of Science (B.Sc.)

vorgelegt von
Johannes Wagner

Referent : *Prof. Dr. Christoph Busch*
Korreferent : *Dr. Christian Rathgeb*

Ausgabedatum: *16.12.2013*
Abgabedatum: *16.03.2014*

Einverständniserklärung

Ich versichere hiermit, dass ich die vorliegende Arbeit selbständig verfasst und keine anderen als die im Literaturverzeichnis angegebenen Quellen benutzt habe. Alle Stellen, die wörtlich oder sinngemäß aus veröffentlichten oder noch nicht veröffentlichten Quellen entnommen sind, sind als solche kenntlich gemacht. Die Zeichnungen oder Abbildungen in dieser Arbeit sind von mir selbst erstellt worden oder mit einem entsprechenden Quellennachweis versehen. Diese Arbeit ist in gleicher oder ähnlicher Form noch bei keiner anderen Prüfungsbehörde eingereicht worden.

Darmstadt, den 14 März 2014

Abstract

Human ears have been used as major feature in the forensic science in recent years. Due to the fact that ear images can be easily taken from distance without knowledge of the examined person, the ear is suitable for security and surveillance use cases. Most surveillance cameras lack in decent image quality for usage with biometric recogniton algorithms. While actual international biometric standards don't consider requirements and guidelines for acquiring ear data, the aim of this thesis is, to build different scenarios with ear image databases[1] for evaluating the image compression impact with state-of-the-art compression standards[2] versus uncompressed image data. In the first step, we compare compressed biometric image sets with ascending quality ordered by compression standard and examine in the second step the robustness of the recognition and detection algorithms at different compression levels/ standards. In the third step we investigate the acuracy of detection and recognition algorithms on scaled images.

In conclusion, this thesis evaluates the optimal choice of compression algorithms and rates for biometric ear images for utilization with ear detection and recognition algorithms.

[1] UND Database (Collection F, Collection G, Collection J2)

[2] JPEG (ISO/IEC IS 109181-1), JPEG 2000 (ISO/IEC IS 15444-1), JPEG XR (ISO/IEC IS 29199-2)

Introduction

The ear as a biometric feature gained a lot attention in recent years. Due to its bigger size compared to other biometric features and the outer ears high visibility makes the ear a proper feature for recognizing persons over a big distance. Thanks to widely used security cameras, indoor and outdoor as well as CCTV camera networks in some countries we often get video material from suspects in criminal cases. While suspects are most likely not looking directly in security cameras or hiding the view to the face wearing basecaps during criminal acts, the ear is often a visible part of their body.
In the year 2000, Hoogstrate et al. from The Netherlands Forensic Institute described a small experiment, examining if a unresolved gas station robbery can be solved by using VHS quality ear pictures captured from the gas stations security camera. 14 years later even bottom-line smartphones provide a better quality compared to VHS.
The problem we face today with captured videos or images is not the lacking quality but rather storage space of the device or transmitting the captured data to an online storage solution with a low mobile bandwidth. For example, the outdated iPhone 4s uses in the vicinity of 3MB per second for HD video and a single image is roughly of size 3MB. With different established lossy and lossless image compression standards we don't know, which format is best suitable in terms of automated ear detection and recognition algorithms.
While ISO/IEC 19794:2013 specifies the image format for iris and other biometric features, except the ear, we have no research about a well suited image format in combination with automated state-of-the-art ear detection and recognition algorithms as well as a investigation about image quality levels for a automated analysis. However, automated biometric recognition systems have a promising application in the future [3] while nowadays forensic applications have only recently started to pay attention on automated ear recognition.
The contribution of this work is the investigation of the effects of different image compression levels and image formats on automated state-of-the-art [5] ear detection and recognition algorithms using appearance features. Considering different reasonable scenarios of data acquision according to surveillance scenarios, full profile pictures and hand cropped ear images of a comprehensive dataset are compressed with lossy and lossless image formats to different quality levels and the performance for detection and recognition is evaluated and analysed.
The remainder of this thesis is organized as follows: in Sect. 2 a introduction to biometrics and used image compression algorithms as well as quality indicators is given. Sect. 3 describes the used materials and software used for experiments in this work and Sect. 4 points out the aquisiton scenarios. Sect. 5 illustrates the experimental setup and how the performance evaluation is done. The results for automated ear recognition and detection are shown in Sect. 6 and are discussed in Sect. 7. Finally conclusions are drawn in Sect. 8

Contents

1 Fundamentals **7**
1.1 Biometric Characteristics . . . 7
1.2 Biometric Systems . . . 7
1.2.1 Enrollment . . . 8
1.2.2 Verification . . . 8
1.2.3 Identification . . . 8
1.2.4 False Accept Rate . . . 8
1.2.5 False Reject Rate . . . 8
1.2.6 Equal Error Rate . . . 8
1.2.7 Detection Error Trade-off . . . 9
1.2.8 Receiver operating characteristic curve . . . 9
1.2.9 Identification Rate . . . 9
1.2.10 Ground Truth . . . 9
1.2.11 Feature Vector . . . 10
1.2.12 Permanence . . . 10
1.2.13 Uniqueness . . . 10
1.3 The Ear as Biometric Identifier . . . 10
1.3.1 Anatomy of the Human Ear . . . 11
1.4 Image Quality . . . 11
1.4.1 PSNR . . . 11
1.5 Image Compression . . . 14
1.5.1 JPEG . . . 14
1.5.2 JPEG2000 . . . 14
1.5.3 JPEG-XR . . . 14

2 Impact of Image Compression on Ear Biometrics **14**
2.1 Materials . . . 14
2.1.1 JJ2000 . . . 14
2.1.2 Microsoft JXR Reference Implementation . . . 15
2.1.3 Imagemagick . . . 15
2.1.4 MATLAB . . . 15
2.1.5 Biometric Databases . . . 15
2.1.6 Normalisation . . . 15
2.1.7 PCA . . . 16
2.1.8 LDA . . . 16
2.1.9 Forced Field Transformation . . . 17
2.1.10 Haar-like Features . . . 17
2.1.11 Adaptive Boost . . . 17
2.1.12 HOG . . . 18
2.1.13 LBP . . . 19
2.1.14 LPQ . . . 21

3 Acquisition Scenarios **21**

4 Experimental Setup **22**
4.0.15 Performance Evaluation – Detection 23
4.0.16 Performance Evaluation – Recognition 24

5 Results **26**
5.1 Results – Detection 26
5.2 Results – Recognition 27

6 Discussion **28**

7 Conclusion **29**

8 Appendix **31**

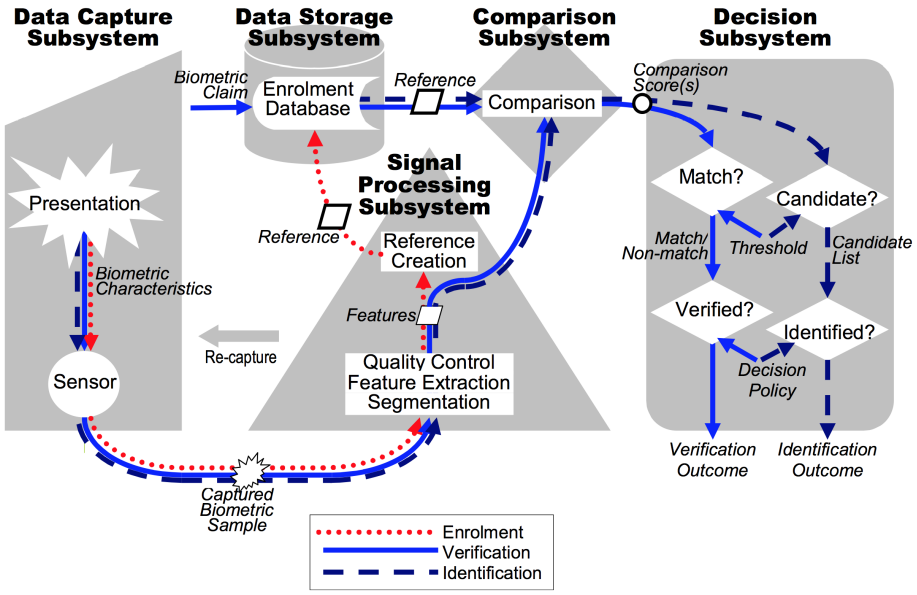

Figure 1: Biometric system in general. Figure taken from [2]

1 Fundamentals

1.1 Biometric Characteristics

Biometric characteristics can be grouped into two categories: biological and behavioral.
Biological: these characteristics can be directly derived from biological features of the human body. Examples for such characteristics include face topography, iris structure and finger topography.
Behavioral: these characteristic can be derived by observing human behaviour. Examples for such characteristics include gait, voice patterns, key-stroke dynamics or handwritten signature dynamics 1.

1.2 Biometric Systems

A System for automated identification or verification of humans with usage of biometric characteristics is defined as a biometric system. The specification standard ISO/IEC JTC1/SC 37 [2] defined five subsystems shown in Fig. 1. The procedure starts with a presentation of a biometric characteristic captured by the Sensor the result is forwarded to the Signal Processing Subsystem where the segmentation of the data sample, the feature extraction and the quality control take place.

1.2.1 Enrollment

For enrolling new subjects, the biometric sample captured by the Sensor runs through the Signal Processing Subsystem, the sample is forwarded to the Data Storage Subsystem, to add the subject to the Enrollment Database and test the verification of the subject against the new template. This routine continues until the subject verification test is successful.

1.2.2 Verification

Verifying a subject is based on a 1:1 comparison between the acquired biometric sample and the database template of the subject. The possible results are acceptance or rejection. A subject is accepted if the comparison score is in the space of the acceptance interval defined by the threshold. Two different system errors can occur, first the false reject error, when the sample of an enrolled subject is rejected and the false accept error, when a sample of a user's identity claim gets accepted with the sample of another person.

1.2.3 Identification

To identify a subject by reference to the biometric sample, a 1:n comparison with the whole or a subset of the database templates takes place. After assembling a candidate list by comparing scores within the specific threshold, the template with the highest score has the sovereign resemblance with the biometric template. Two different errors can happen, first, the false negative error, if an enrolled subjects template is not on the candidate list and second, the false positive error if a sample gets on the candidate list without being enrolled.

1.2.4 False Accept Rate

The *false accept rate* (FAR) metes the ratio of subjects, whose identity claims were aberrant accepted by the biometric system. This error rate cannot be determined in a production system without checking the identity of a subject two times, because there is no solution to detect false acceptance in an automated verification scenario.

1.2.5 False Reject Rate

The *false reject rate* (FRR) metes the ratio of enrolled users, whose identity claim was rejected by the biometric system. The FRR can only be determined by evaluating the reason for the reject in a generative system, since the identity claim reject might be valid e.g. due to the expiration of an identity document.

1.2.6 Equal Error Rate

The *equal error rate* (EER) is defined as the setting where FAR and FRR are equal and can be visualised in a detection Error-Trade-off (DET) curve. This metric is important for the evaluation of a biometric system, as it represents the lowest achievable total error by balancing convenience (low FRR) and security (low FAR).

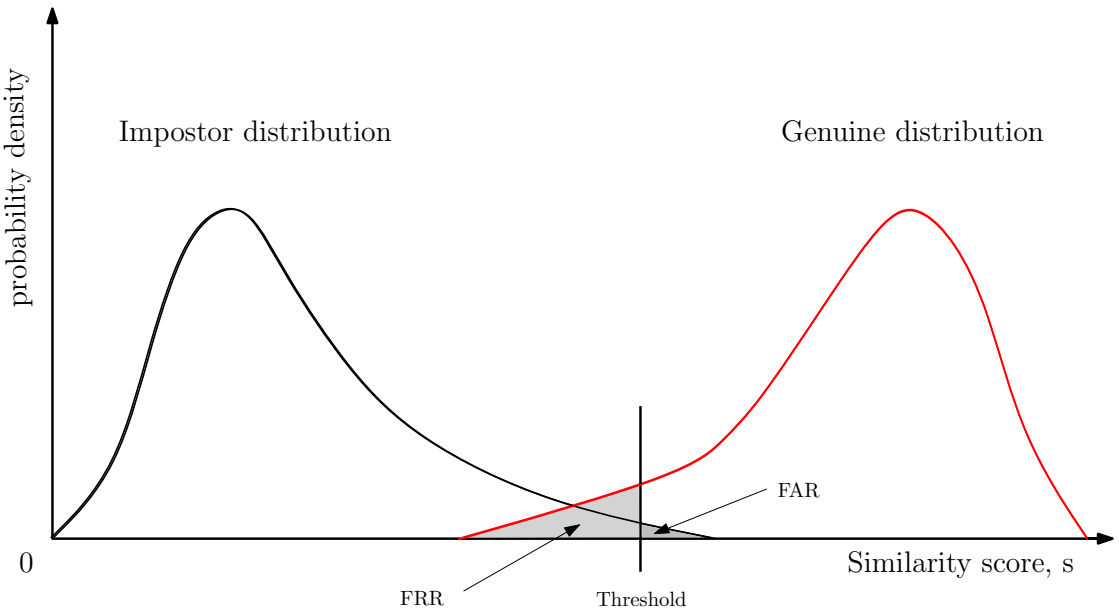

Figure 2: Receiver Operator Characteristics Curve

1.2.7 Detection Error Trade-off

Detection Error Trade-off (DET) is the graph of *False Accept Rate* vs *False Reject Rate*, which is obtained by varying the system parameters such as match threshold [13].

1.2.8 Receiver operating characteristic curve

Receiver operating characteristic curves (ROC curves) are often plotted using logarithmic axes to better differentiate the systems that shows similar performance [13]. Fig. 2 shows the FRR and the FAR in a ROC curve.

1.2.9 Identification Rate

Identification Rate (IR) is the proportion of identification operations by subjects enrolled in the system where the corresponding identifier is the one returned by the system.

1.2.10 Ground Truth

In machine learning, the *ground truth* refers to the accuracy of the training sets classification for superintended learning techniques. In our work the ground truth refers to an by hand annotated

profile image for every single image in the test dataset. This mask was also used for cropping the Region of Interest, i.e. the ear for the biometric recognition.

1.2.11 Feature Vector

In pattern recognition and machine learning, a *feature vector* is an n-dimensional vector of numerical features that represent some object. A lot of machine learning algorithms require a numerary translation of objects, since such representations facilitate processing and statistical analysis. When representing images, the feature values might correspond to the pixels of an image. Feature vectors are equivalent to the vectors of explanatory variables used in statistical procedures such as linear regression. Feature vectors are often combined with weights using sums or products in order to construct a linear predictor function that is used to determine a score for making a comparison possible.

1.2.12 Permanence

Permanence refers to the extent to which the attribute does not change over time. The fingerprint and the ear are very persistent, hardly changing at all throughout adulthood. The face and the iris are much less persistent, one changing with expression and the other responding to changes in ambient lighting. Other less persistent biometrics include speech or gait [6].

1.2.13 Uniqueness

Uniqueness is how unlikely a description is to occur more than once in the population. The iris is believed to be one of the most unique biometrics. As mentioned with fingerprints, the degree of uniqueness will also depend on the number of fingers being considered [6].

1.3 The Ear as Biometric Identifier

Alphonse Bertillon, a french criminal investigator and anthropologist developed a anthropometric system for human identification called Bertillonage [8] as one of the earliest systems of measurement and recording personal characteristics which includes the length of the ear as an anthropometric indicator. Another prominent user of the ear as biometric is Alfred V. Iannarelli. He is an consultant in criminal investigation and forensics who developed a system of ear classification for the American law enforcement agencies which is called Iannrelli System of Ear Identification [9].

> *" The ear, thanks to these multiple small valleys and hills that plough across it, is the most important factor from the point of view of identification. Immutable in its form since birth, resistant to the influences of environment and education, this organ remains, during the entire life, like the intangible legacy of heredity and life in the womb. "*
>
> Alphonse Bertillon
> Legal photography, Paris, Gauthier-Villars, 1890

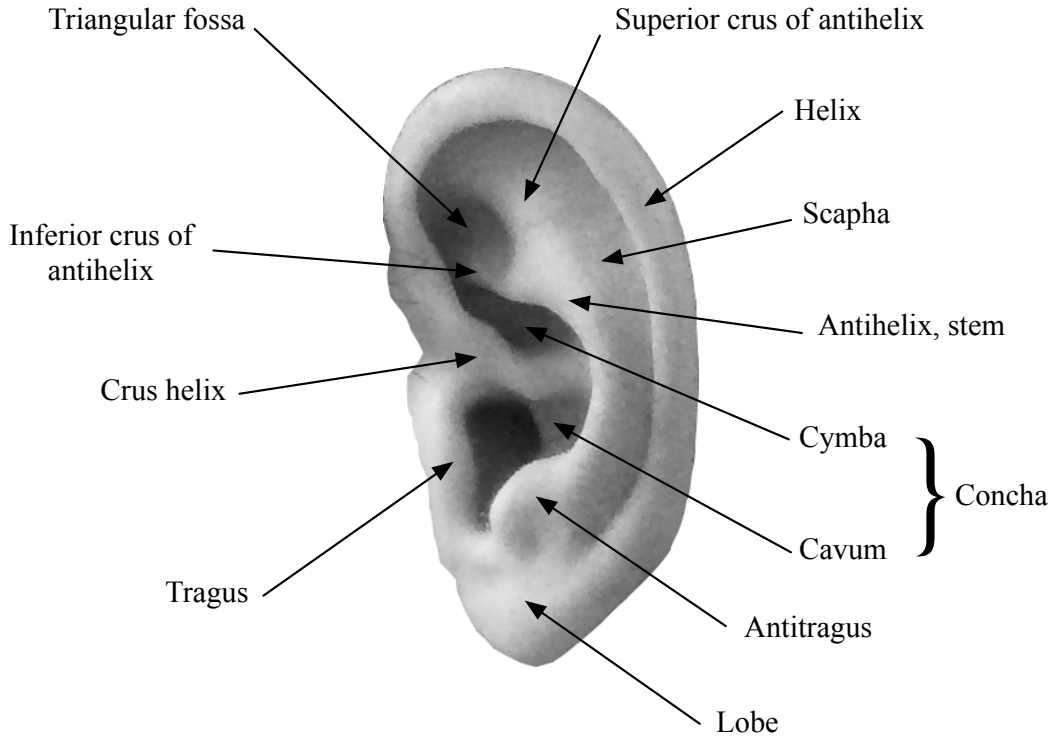

Figure 3: Anatomy of the human ear anatomical landmarks

Regarding the great visibility and size, the human ear is a suitable biometric feature in case of surveillance scenarios or difficult circumstances like bad lightning conditions in combination with large distances or bad sample quality [20]. Table 1 shows an overview about permanence on several biometric features

1.3.1 Anatomy of the Human Ear

The human ear comprises standard biometric features like the face. These include the helix and the antihelix and other anatomical regions suitable for feature extraction. Fig. 3 shows the locations of the anatomical landmarks in detail.

1.4 Image Quality

1.4.1 PSNR

Peak signal-to-noise ratio or PSNR, is an expression for the proportion between the maximum strength of a signal and the power of blight noise that affects the precision of its representation. Concerning the wide dynamic range of many signals, PSNR is usually enunciated in terms of the

Table 1: Comparison of various biometric technologies

High, Medium, and Low are denoted by H, M, and L [4]

Biometric identifier	Universality	Distinctiveness	Permanence	Collectablility	Performance	Acceptability	Circumvention
DNA	H	H	H	L	H	L	L
Ear	M	M	H	M	M	H	M
Face	H	L	M	H	L	H	H
Facial thermogram	H	H	L	H	M	H	L
Fingerprint	M	H	H	M	H	H	M
Gait	M	L	L	H	L	H	M
Hand geometry	M	M	M	H	M	M	M
Hand vein	M	M	M	M	M	M	L
Iris	H	H	H	M	H	L	L
Keystroke	L	L	L	M	L	M	M
Odor	H	H	H	L	H	L	L
Palmprint	M	H	H	M	H	M	M
Retina	H	H	M	L	H	L	L
Signature	L	L	L	H	L	H	H
Voice	M	L	L	M	L	H	H

logarithmic decibel scale. PSNR is most commonly used to measure the quality of reconstruction of lossy compression codecs like JPEG. In our experiments the signal is the original image and noise refers the error precipitated by compression. PSNR is only conclusively valid when it is used to compare results from the same image like uncompressed database sample versus the compressed version of the same image.
Prestigious values for the PSNR on compressed images are between 30 and 50 dB. In our experiments, we use PSNR to quantify the resulting image quality.
As nuisance value the Mean Square Error (MSE) is used. For two $m \times n$ black and white images I for the original image and K for a degraded image the MSE is defined as:

$$\mathrm{MSE} = \frac{1}{mn} \sum_{i=0}^{m-1} \sum_{j=0}^{n-1} (I(i,j) - K(i,j))^2 \tag{1}$$

PSNR is defined as:

$$\mathrm{PSNR} = 10 \cdot \lg \frac{I_{\max^2}}{\mathrm{MSE}} \,\mathrm{dB} = 20 \cdot \lg \frac{I_{\max}}{\sqrt{\mathrm{MSE}}} \,\mathrm{dB} = (2 \cdot \lg I_{\max - \lg \mathrm{MSE}) \cdot 10 \,\mathrm{dB}} \tag{2}$$

I_{max} is the maximum pixel value, e.g. for 8 Bit the maximum pixel value is 255

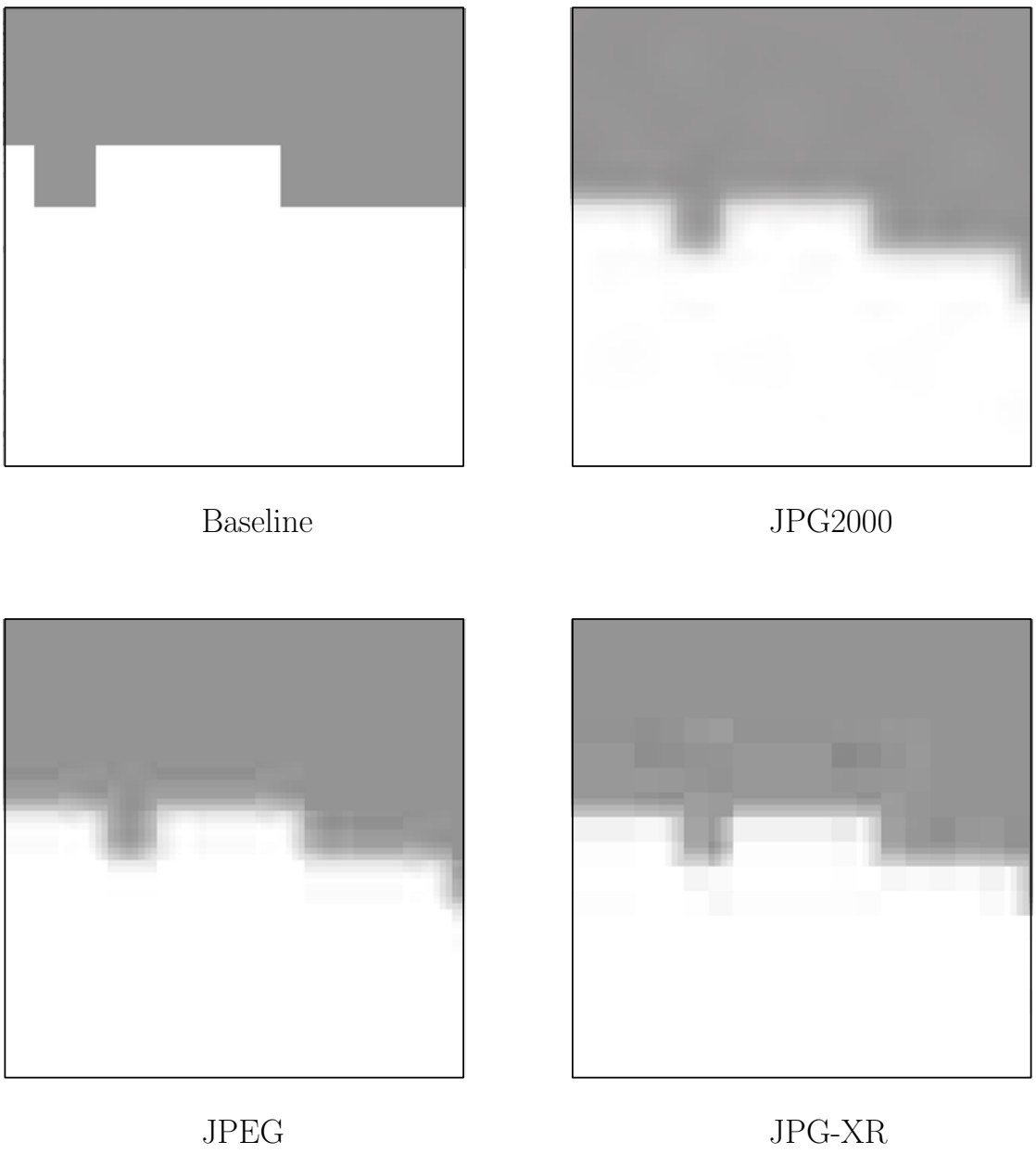

Figure 4: Artifacts for different image compression formats

1.5 Image Compression

1.5.1 JPEG

JPEG is an lossy image compression standard specified in [17], based on the discrete cosine transform. It divides an image in separate 8×8 segments which can be visible when the compression rate is elevated. The RGB or CMYK color values are converted to a luminance/ chrominance color space, i.e. YUV. The compression level is set due transformation tables to quantize the DCT coefficients. Finally the resulting data is compressed by a lossless Huffman encoding for reducing image file size.

1.5.2 JPEG2000

JPEG2000 as defined in [16] is an wavelet-based image compression standard developed by the Joint Photographic Experts Group in the year 2000 with lossless compression support and less visible artifacts as well as superior compression performance compared to the JPEG standard from 1992. While JPEG produces blocking artifacts, JPEG2000 produces so called ringing artifacts shown in Fig. 4.

1.5.3 JPEG-XR

JPEG extended range is an image compression standard developed by Microsoft® and specified in [18] which supports both lossy and lossless image compression. The architecture is very similar to the JPEG architecture. JPEG-XR uses a two-level transformation with 16×16 macroblocks and a 4×4 core transformation. To reduce artifacts at low bitrates, JPEG-XR provides a optional overlap prefiltering step before the two-level transformation. The discrete cosine transformation used in JPEG-XR is invertible (lossless). The JPEG-XR library is licensed under the BSD license.

2 Impact of Image Compression on Ear Biometrics

2.1 Materials

2.1.1 JJ2000

JJ2000[3] is an open source JPEG2000 encoder/ decoder written in Java and used in our experiments for compressing image data with JPEG2000. JPEG2000 and the JJ2000 implementation support the image compression to a specified bit per pixel value. We use this tool in combination with a bash script to convert our self-composed imageset to predefined bitrates from 0.1 bpp – 1.0 bpp

[3] https://code.google.com/p/jj2000/

2.1.2 Microsoft JXR Reference Implementation

T.JXR-1[4] released by MicrosoftMicrosoft® under the Microsoft Open Specification Promise[5] is the reference implementation of JPEG-XR developed by Microsoft®. in experiments, the reference software is utilized with a python script which calculates the current bit per pixel of an image due to the file size minus standard header, for achieving our predefined bit rates on the self-composed imageset.

2.1.3 Imagemagick

Imagemagick is an Open Source software suite for converting and editing image files. Part of Imagemagick are command line tools for converting and manipulating images who are applicable for usage with scripting languages or batch converting. For converting images to a specified bit per pixel rate, we developed a script in Python which iterates the quality parameter and calculates the bpp with file size without standard header and image resolution, until the resulting image achieved the predefined rate. The software can be found on the Internet[6].

2.1.4 MATLAB

MATLAB® is a commercial computing environment and programming language widely used in academic and research institutions as well as industrial enterprises. The algorithms described in Sect. 4 are part of the biometric framework developed by Anika Pflug or part of the MATLAB® Image Processing Toolbox.

2.1.5 Biometric Databases

Experimental results are conducted on the 2D images from the UND Biometrics Database collected between 2003 and 2005 by the University of Notre Dame[7]. For evaluation we used a self-composed dataset which contains 2369 left profile images from 510 human subjects from the database subsets:

- *Collection G* [23], with 738 2D profile images from 302 human subjects
- *Collection J2* [22], with 1800 2D profile images from 415 human subjects
- *Collection NDOff-2007* [21], with 7398 2D images from 396 human subjects with different yaw and pitch poses described by the file names

2.1.6 Normalisation

Using a self-composed dataset made of different database collections requires a contrast normalisation step to get a homogeneous database. Therefore we normalize the images with the

[4] http://www.itu.int/rec/T-REC-T.835
[5] http://www.microsoft.com/openspecifications/en/us/programs/osp/default.aspx
[6] http://www.imagemagick.org/
[7] https://www.nd.edu/

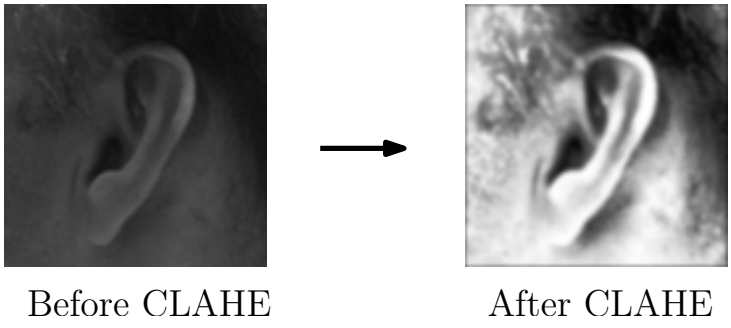

Figure 5: sample image before and after CLAHE application

Contrast-limited Adaptive Histogram Equalization (CLAHE) algorithm. CLAHE works on tiles instead to the whole image at once. resulting tiles are combined with an interpolation step to eliminate artificially induced boundaries afterwards. Fig. 5 shows the difference after the CLAHE application with a database sample.

2.1.7 PCA

Principal Component Analysis (PCA) is a technique for finding patterns in high dimensional data and often used in face recognition that uses orthogonal transformation to convert a set of observations of possibly correlated variables into a set of values of linearly uncorrelated variables called principal components.
This technique searches for directions in the data that have largest variance and subsequently project the data onto it. In this way, we obtain a lower dimensional representation of the data, that removes some of the ”noisy” directions. Principal Component Analysis is an unsupervised technique and as such does not include label information of the data. The basic approach is to compute the eigenvectors of the covariance matrix, and approximate the original data by a linear combination of the leading eigenvectors.

2.1.8 LDA

Linear Discriminant Analysis (LDA) also known as *Fisher's Linear Discriminant* (FLD), is a method used in statistics, pattern recognition and machine learning to find a linear combination of features before classification which characterizes or separates two or more classes of objects or events. The resulting combination may be used as a linear classifier, or, more commonly, for dimensionality reduction before later classification. LDA is closely related to PCA to look for linear combinations of variables which best explain the data. LDA explicitly attempts to model the difference between the classes of data. Compared to PCA, LDA does not take into account any difference in class, and factor analysis builds the feature combinations based on differences

rather than similarities. The goal of LDA is to reduce dimension of feature vectors without loss of information.

2.1.9 Forced Field Transformation

Forced Field Transformation (FFT) reduces the dimensionality of pattern space maintain the discriminatory power for classification and invariant description. Compared to Sobel edge detection, the FFT leads in well detected textures, more features, sharper edges and profits from thresholding.

benefits of the Forced Field Transformation are a simplified implementation in the time domain and time complexity is reduced considerably by working in frequency domain but it is difficult to implement it in frequency domain. While providing high computational costs using direct method, the efficiency compared to other techniques is higher but not widely applicable.

2.1.10 Haar-like Features

Haar-like features are digital image features widely used in object recognition. Historically, working with only image intensities, i.e. the RGB pixel values at each and every pixel of image made the task of feature calculation computationally expensive. A publication by Papageorgiou et al. [7] discussed working with an alternate feature set based on Haar wavelets instead of the usual image intensities. Viola and Jones adapted the idea of using Haar wavelets and developed the so-called Haar-like features. A Haar-like feature considers adjacent rectangular regions at a specific location in a detection window, sums up the pixel intensities in each region and calculates the difference between these sums. This difference is then used to categorize subregions of an image. For example, let us have an image database with human faces. It is a common observation that among all faces the region of the eyes is darker than the region of the cheeks. Therefore a common Haar feature for face detection is a set of two adjacent rectangles that lie above the eye and the cheek region. The position of these rectangles is defined relative to a detection window that acts like a bounding box to the target object in Fig. 8 (the eyes in this case).

2.1.11 Adaptive Boost

Adaptive Boost (AdaBoost) is a machine learning algorithm which was proposed in 1995 by Yoav Freund and Robert Schapire as a method for generating a strong classifier out of a set of weak calssifiers. It is used for improved accuracy in combination with pattern recognition classifiers. A well-known combination is Haar-like features combined with an AdaBoost training.
AdaBoost reduces the amount of features by the use of only selecting features who are useful those are called weak classifier. It eliminates redundant and useless features depending on the shape of the object which should be detected and assembles a strong classifier and reduces the computational costs for the addition instruction for calculating the sum's of the black and white feature-grids by building an integral image. AdaBoost uses cascading, which basically is applying different window sizes for features on a single image to improve feature performance Fig. 7 shows a general procedure of the Sliding-Window technique.

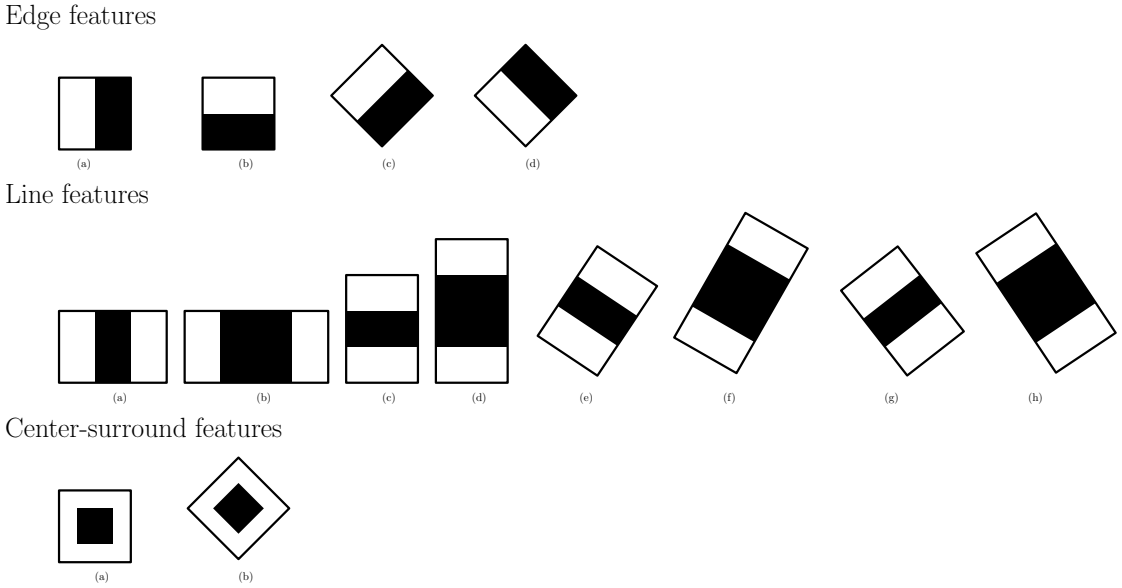

Figure 6: Haar-like Feature types

2.1.12 HOG

Histogram of Oriented Gradients (HOG) is a feature descriptor widely used in computer vision for the purpose of object detection. HOG counts incidents of gradient orientation in local tiles of an image. The major thought behind HOG is that local object shape inside an image can be described by the distribution of intensity gradients or edge directions. A implementation of the HOG descriptor can be done by separating the image into small tiles, the cells, and composing a histogram of gradient directions or edge orientations for the pixels within the cell shown in Fig. 9 for each cell. The concatenation of the cell histograms represents the descriptor. For improved accuracy, the local histograms can be normalized by calculating a measure of the intensity across a larger region of the image, called a block, and then use this value to normalize all cells within the block. This normalization results in better invariance to changes in illumination or shadowing. The HOG descriptor has a few advantages over other descriptor principles. Since the HOG descriptor operates on localized cells, the method upholds invariance to geometric and photometric transformations, except for object orientation. Such changes would only appear in larger spatial regions. Moreover, as Dalal and Triggs discovered, coarse spatial sampling, fine orientation sampling, and strong local photometric normalization permits the individual body movement of pedestrians to be ignored so long as they maintain a roughly upright position. The HOG descriptor is thus particularly suited for human detection in images[10].

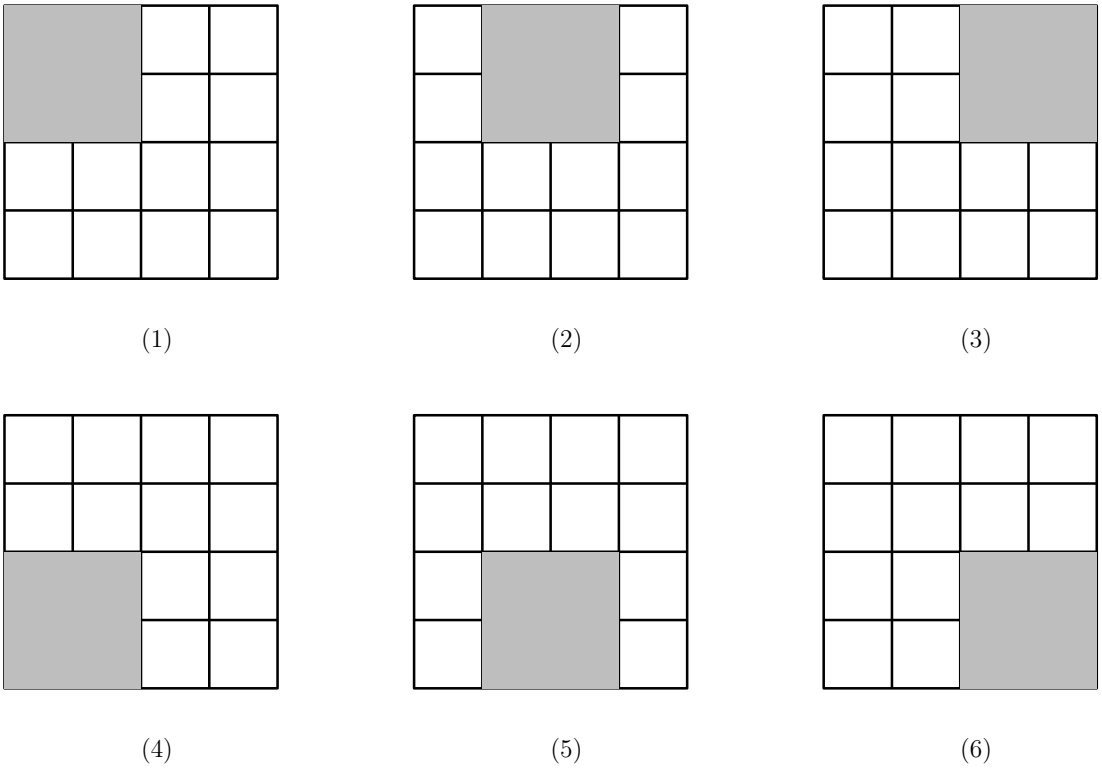

Figure 7: Sliding-Window searching for features

2.1.13 LBP

Local Binary Patterns (LBP) is a simple and very efficient texture operator which labels the pixels of an image by thresholding the neighborhood of each pixel and considers the result as a binary number. Due to its discriminative power and computational simplicity, the LBP texture operator has become a popular approach in various applications. It can be seen as a unifying approach to the traditionally divergent statistical and structural models of texture analysis. Perhaps the most important property of the LBP operator in real-world applications is its robustness to monotonic gray-scale changes caused, for example, by illumination variations. Another important property is its computational simplicity, which makes it possible to analyze images in challenging real-time settings [12]. The basic idea behind LBP is that an image is composed of micropatterns. LBP is the first order circular derivative of patterns that is generated by concatenating the binary gradient directions. A histogram of these micropatterns contains information about the distribution of edges and other local features in an image. In our experiments, we use the full profile images cropped to 100×100 by reference to the ground truth mask, before we apply the feature extraction.

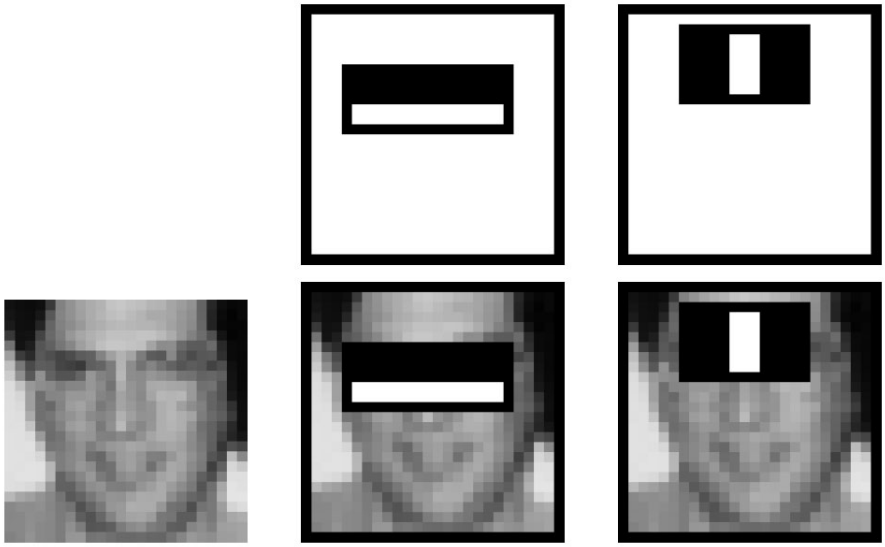

Figure 8: first two features selected by AdaBoost for eye detection from [15]

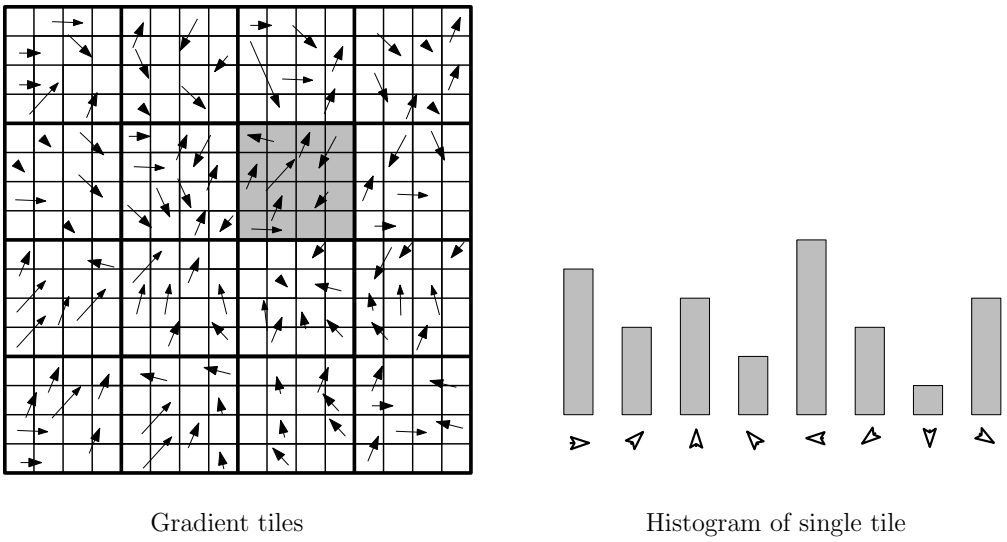

Figure 9: Local gradients converted to histogram

The conventional LBP operator extracts information that is invariant to local grayscale variations in the image.
It is computed at each pixel location, considering the values of a small circular neighborhood around the value of a central pixel. Fig. 10 illustrates the process binarizing an image tile through a threshold and concatenating to a feature vector afterwards.

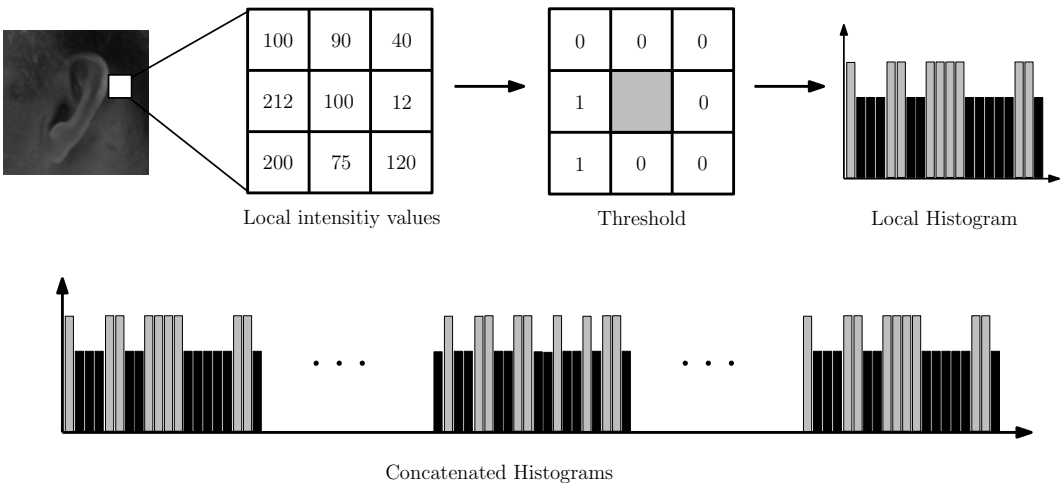

Figure 10: Concatenated local binary patterns, binarized by threshold

2.1.14 LPQ

The *Local Phase Quantization* (LPQ) operator was originally proposed by Ojansivu and Heikkila [11] as a texture descriptor.
LPQ is based on the blur invariance property of the Fourier phase spectrum. It uses the local phase information extracted using the 2-D short-term Fourier transform (STFT) computed over a rectangular neighborhood at each pixel position of the image. In LPQ only four complex coefficients are considered, corresponding to 2-D frequencies. The quantized coefficients are binary encoded from 0-255. Finally, a histogram is composed and used as an 256-dimensional feature vector. In our experiments, we use the full profile images cropped to 100×100 by reference to the ground truth mask, before we apply the feature extraction step.

3 Acquisition Scenarios

Table 2 summarizes different state-of-the-art surveillance cameras made available by major vendors and relevant characteristics, i.e. focal length, resolution, and sensor type (characteristics refer to currently best products). Based on this comparison we simulate a camera providing (1) a focal length of 8mm, (2) a resolution of 1920×1080, and (3) a sensor diagonal of 1/2.5 inch. We examine two different acquisition scenarios $\mathcal{S}_1$, $\mathcal{S}_2$ with respect to the distance of the subject to the camera considering distances of 2m and 4m, respectively. Fig. 11 schematically depicts the considered acquisition scenario.

Let $C(f, d, w, h)$ be a camera with focal length f, sensor diagonal d, and resolution $w \times h$. Then

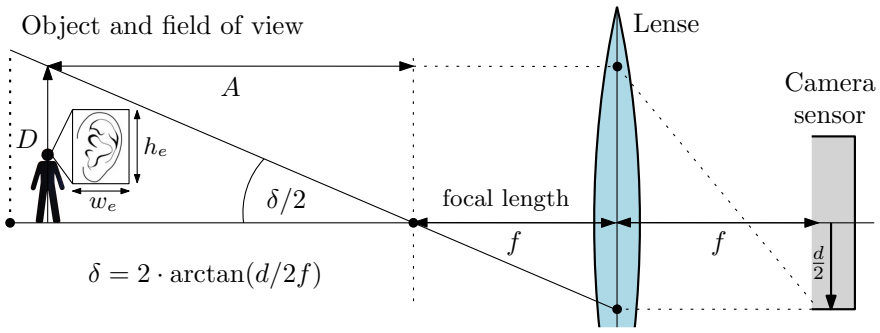

Figure 11: Simulated data acquisition scenario.

the diagonal D of the field of view at a distinct distance A is estimated as,

$$\begin{aligned} D = &\ A \cdot \tan(2 \cdot \arctan((d/2f)/2)) \\ = &\ A \cdot d/2f \end{aligned} \tag{3}$$

In our scenario the aspect ratio is 16:9, i.e. the field of view in object space corresponds to

$$16 \cdot \sqrt{D^2/(16^2 + 9^2)}\ \mathrm{m} \times 9 \cdot \sqrt{D^2/(16^2 + 9^2)} \tag{4}$$

In [19] the average size of the outer ear of males and females across different age group is measured as $61.7mm \times 37.0mm$ and $57.8mm \times 34.5mm$, respectively. For an average angle of auricle of 32.5 degrees across age groups and sex we approximate the bounding box of an ear of any subject as 70 mm × 60 mm. For both scenarios $\mathcal{S}_1$, $\mathcal{S}_2$ the considered camera C(8mm, 1/2.5”, 1920px, 1080px) would yield images where ear regions comprise approximately $w_e \times h_e = 110 \times 90$ and 55×45 pixels, respectively.

4 Experimental Setup

The experimental setup is shown in Fig. 11. We suppose that we are able to identify a subject in a video, captured by a state-of-the-art surveillance camera listed in 2. After prosperous segmenting the outer ear with algorithms described in Sect. 2.1 we analyse feature extraction with techniques from Sect. 2.1 on 100×100 cropped and 50% scaled 50×50 images. The cropped images are based on the ground truth coordinates given by the hand annotated ground truth data.
The source of the used images is a self-composed imageset containing to the UND Database and is degraded by lossy and lossless compression formats, i.e. JPEG, JPEG2000 and JPG-XR with compression rates leading to 1.0 – 0.1 Bits per pixel. The Bits per pixel are determined by continuously incrementing the compression value, i.e. 0 – 100 on the grayscaled images, implemented by a self written Python script with application of the Imagemagick python bindings by dividing the filesize deducting the standard image format header and the product of image height and width. JPEG2000 provides compression by stating the bits per pixel. The image

quality was examined by measuring the mean Peak to Signal Noise Ratio (PSNR) of the separate datasets by utilization Imagemagick command line tools automated with a Bash script. Since Matlab lacks in supporting JPEG-XR, the images are converted back to the PNG format after compressing them with the formats from Sect. 2.1. Fig. 12 shows the compression results on a sample image with different compression algorithms on 0.1 bpp compression rate and Fig. 13 shows the effects of compression on the segmented ear area on 0.2 bpp for the used compression formats as well as the original image.

Table 2: State-of-the-art camera models and characteristics.

Vendor	Product	Focal length	Resolution	Sensor
ACTi[1]	D82	2.8-12mm	1920×1080	1/3.2”
AXIS[2]	P3367V	3-9mm	1920×1080	1/3.2”
GeoVision[3]	GV-FD220G	3-9mm	1920×1080	1/2.5”
Veilux[4]	VVIP-2L2812	2.8-12mm	1920×1080	1/2.5”

[1] http://www.acti.com/
[2] http://www.axis.com/
[3] http://www.geovision.com.tw/
[4] http://www.veilux.net/

4.0.15 Performance Evaluation – Detection

Biometric feature extraction requires segmenting the ear region from the whole image beforehand. We crop the detected ear region out of the full profile image with regards to the ground truth mask. To reduce time in Enrollment and on big image databases we fall back on image processing algorithms to segment a ”Regoin of interest”.
For improving detection performance, we use AdaBoost classifier with Haar-like features trained with test images from the WPUT ear database for positives and negative images from the INIRA person detection dataset [24] based on Haar-like features described by [15] also HOG and LBP. The automated detection result is a black image called mask with the same resolution as the input image and a whitened out ear section if the classifier was able to detect something. Comparing the automatically generated image mask to the hand annotated ground truth image, which represents a perfect detection result, leads in the grade of not overlapping detected pixels. Due to the black and white pixels in the image represented by 0 and 1, we calculate the grade of overlapping with *XOR* operation, measuring the non overlapping pixels from the ground truth mask shown in Fig. 14 divided by the size of ground truth mask’s height and width. X_i refers to the resulting error while G_i represents the ground truth congregation and E_i the portion of the examined picture i. E_{ih} and E_{iw} refers to height and width of the ground truth mask.

$$X_i = \frac{|G_i \oplus E_i|}{|G_{ih}| \times |G_{iw}|} \qquad \mathrm{X}_i \in [0, 1] \tag{5}$$

For experiments, we used the MATLAB® implementation of these referenced algorithms from

(a) Original | 100%

(b) J2K | 0.1 bpp

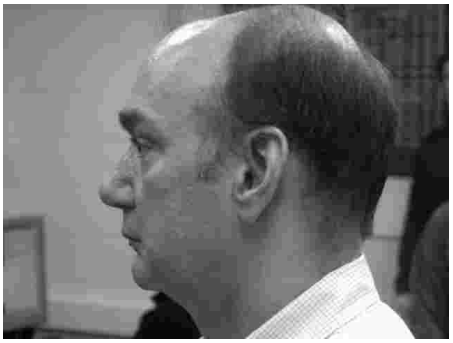

(c) JPG | 0.1 bpp

(d) J-XR | 0.1 bpp

(e) Original | 50%

(f) J2K | 0.1 bpp

(g) JPEG | 0.1 bpp

(h) J-XR | 0.1 bpp

Figure 12: Maximum compression with JPEG2000, JPEG and JPEG-XR $\mathcal{S}_1$ (b)-(d) and $\mathcal{S}_2$ (f)-(h) for full profile images (a) and (e) on sample image `ID_02463d677` of the UND dataset.

the "Image Processing Toolbox", which can be found on the Internet[8].

4.0.16 Performance Evaluation – Recognition

To assess recognition performance we use the classifiers from detection appendixed by LPQ features with a CLAHE normalisation procedure beforehand concerning the self-composed imageset generated from different subsets of the UND Database used for evaluation. All performance indi-

[8] http://www.mathworks.com/products/image/

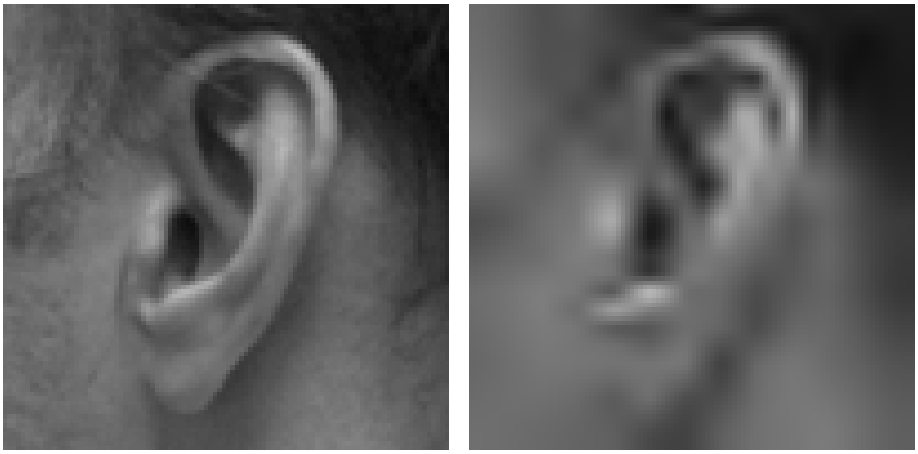

(a) Original|100%

(b) J2K | 0.2 bpp

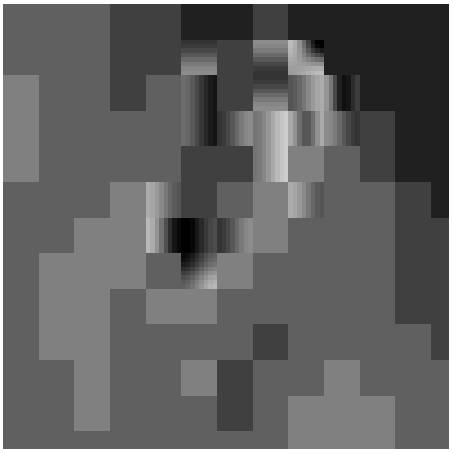

(c) JPG | 0.2 bpp

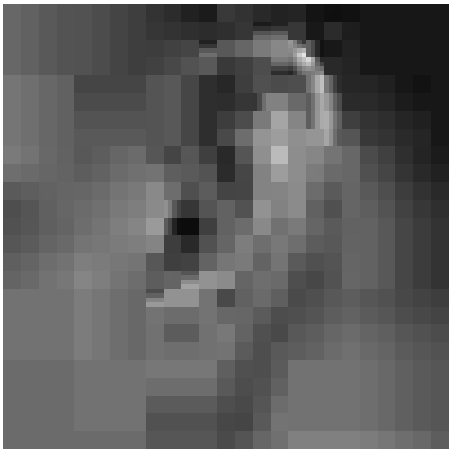

(d) J-XR | 0.2 bpp

(e) Original | 50%

(f) J2K | 0.2 bpp

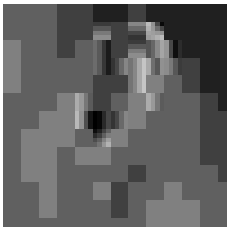

(g) JPEG | 0.2 bpp

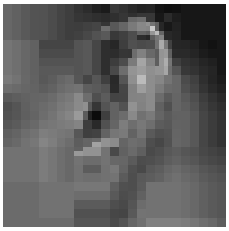

(h) J-XR | 0.2 bpp

Figure 13: High compression with JPEG22000, JPEG and JPEG-XR $\mathcal{S}_1$ (b)-(d) and $\mathcal{S}_2$ (f)-(h) for cropped images (a) and (e) on sample image `ID_02463d677` of the UND dataset.

cators for recognition are median values based on a five-fold cross validation. The performance for recognition is measured by the Equal Error Rate (EER) and the Identification Rate (IR). In

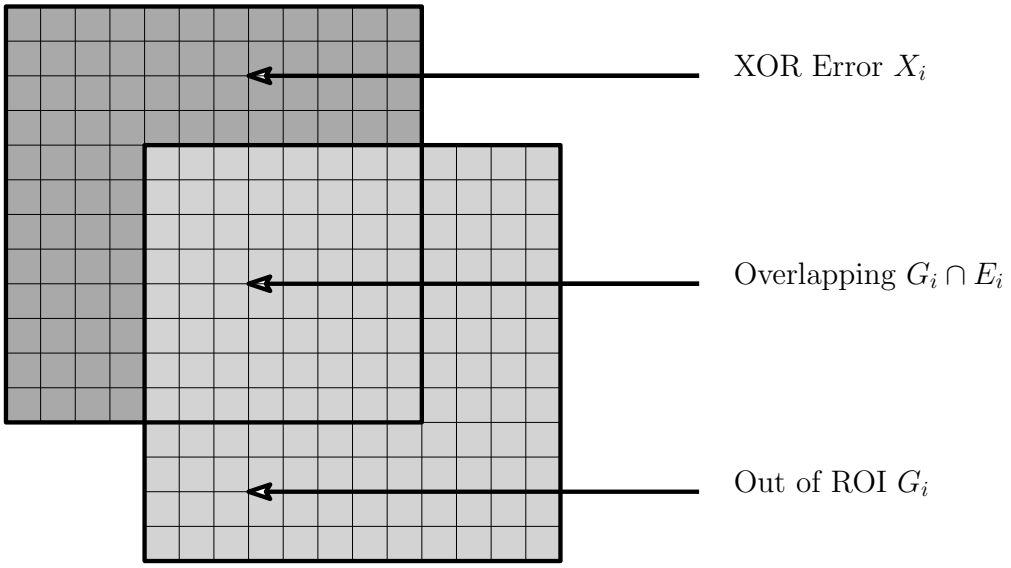

Figure 14: Sample regions in error calculation

this work identification is performed in the closed-set scenario returning the rank-1 candidate as identified subject (without applying a decision threshold).

5 Results

5.1 Results – Detection

Table 3 summarizes the biometric performance with respect to error rates for different detection algorithms and compression intensities of JPEG, JPEG200 and JPEG-XR for both advised scenarios. The quality of generated images is estimated in terms of average PSNR. Table 3 illustrates the change of biometric performance according to the applied intensities of image compression. Experimental results indicate that the detection classifiers did not profit from the lossless compression in $\mathcal{S}_1$ as well as in $\mathcal{S}_2$. Even with higher bit per pixel rates, the accuracy for lossless compression is marginal. Table 3 shows the sweet spot in between 0.6bpp - 1.0bpp. HOG with not relying on edge detection and LPQ, deliver the best performance followed by Haar-like features. Due to the artifact pixels in the neighborhood for JPEG-XR and the blur-like smoothness JPG2000 produces, the lossless image compression formats deliver a significant inferior performance compared to JPEG. The experiments show, that the softness of the edges are more a problem than artifact pixel in the edge area. This suggest that small amounts of artifact pixel can be compensated contrary to a blurred edge. The sliding-window observes neighborhood for finding patterns with bright to dark transitions as well as gradients. The results also show, that PSNR isn't a suitable measurement for predicating sufficient image quality in a automated

Table 3: Error rates for different detection algorithms for both scenarios (errors have been multiplied by 10^2). X_1, X_2, X_3 represent the feature types Haar, LBP and HOG

		Scenario S_1				Scenario S_2			
Format	**bpp**	**PSNR**	X_1	X_2	X_3	**PSNR**	X_1	X_2	X_3
PNG	–	∞	2.12	2.86	1.94	∞	2.64	2.75	1.97
J2K	0.1	37.15 db	6.70	6.84	7.06	41.25 db	6.47	6.2	7.16
J2K	0.2	38.86 db	6.75	6.95	7.07	44.11 db	6.4	6.33	7.17
J2K	0.3	39.82 db	6.78	6.96	7.07	45.20 db	6.47	6.31	7.11
J2K	0.4	40.36 db	6.79	6.92	7	45.73 db	6.54	6.34	7.13
J2K	0.5	40.95 db	6.69	6.79	6.95	46.24 db	6.51	6.35	7.23
J2K	0.6	41.43 db	6.77	6.79	6.77	46.04 db	6.52	6.31	7.15
J2K	0.7	41.86 db	6.68	6.73	6.81	46.09 db	6.49	6.35	7.18
J2K	0.8	42.29 db	6.75	6.74	6.82	46.14 db	6.5	6.36	7.17
J2K	0.9	42.73 db	6.77	6.72	6.83	46.20 db	6.49	6.39	7.14
J2K	1.0	43.21 db	6.79	6.65	6.8	46.25 db	6.49	6.38	7.18
JPG	0.1	34.60 db	4.13	3.4	4.29	36.69 db	5.51	3.43	5.6
JPG	0.2	37.41 db	3.24	2.24	3.13	41.26 db	3.72	2.29	4.16
JPG	0.3	38.66 db	2.89	2.12	2.6	43.51 db	3.12	2.03	3.25
JPG	0.4	39.30 db	2.67	2.12	2.17	44.70 db	2.98	1.98	2.89
JPG	0.5	39.78 db	2.59	2.1	2.11	45.39 db	2.84	1.96	2.83
JPG	0.6	40.21 db	2.7	2.09	2.15	45.83 db	2.71	1.96	2.77
JPG	0.7	40.42 db	2.62	2.09	2.13	46.14 db	2.82	2.02	2.76
JPG	0.8	40.87 db	2.67	2.09	2.13	46.35 db	2.81	2	2.76
JPG	0.9	41.11 db	2.71	2.1	2.13	46.49 db	2.82	2.02	2.74
JPG	1.0	41.39 db	2.74	2.09	2.13	46.58 db	2.93	2.04	2.8
JXR	0.1	35.03 db	6.66	6.3	7.15	37.68 db	6.38	6.7	7.06
JXR	0.2	37.01 db	6.66	6.55	7	40.74 db	6.52	6.42	7.17
JXR	0.3	38.37 db	6.65	6.62	7	42.41 db	6.45	6.42	7.18
JXR	0.4	39.07 db	6.68	6.6	6.97	43.46 db	6.57	6.42	7.14
JXR	0.5	39.64 db	6.7	6.66	6.92	44.15 db	6.52	6.44	7.14
JXR	0.6	40.23 db	6.7	6.74	6.97	44.59 db	6.48	6.42	7.19
JXR	0.7	40.64 db	6.69	6.74	6.96	44.95 db	6.45	6.39	7.21
JXR	0.8	41.21 db	6.68	6.69	6.87	45.23 db	6.45	6.43	7.19
JXR	0.9	41.47 db	6.63	6.67	6.82	45.43 db	6.48	6.39	7.16
JXR	1.0	41.70 db	6.6	6.62	6.78	45.64 db	6.51	6.42	7.14

biometric system. The improvements concerning average PSNR rates on 100% scaled as well as on 50% scaled images on higher bpp rates, we have mostly the same performance for detection as well as for recognition. Sec. 8 presents the results visualy rehashed.

5.2 Results – Recognition

Table 4 summarizes the biometric performance concerning to EERs and IRs for different feature extraction algorithms on JPEG, JPEG200 and JPEG-XR compressed data for both advised scenarios. The quality of generated images is estimated in terms of average peak signal to noise ratio (PSNR). Sect. 8 illustrates the Equal Error Rates (EER) and Identification Rates (IR) for different scenarios.

Table 4: Equal error rates and true-positive identification rates for different algorithms and scenarios.

Format	bpp	Scenario S_1	LBP		LPQ		HOG		Scenario S_2	LBP		LPQ		HOG	
		PSNR	EER	IR	EER	IR	EER	IR	PSNR	EER	IR	EER	IR	EER	IR
PNG	None	∞	1.22	96.75	0.13	99.74	4.80	87.40	∞	4.1	86.49	1.06	97.14	4.87	85.58
J2K	0.1	19.85 db	45.58	6.62	45.81	6.49	42.06	5.19	19.98 db	44.90	6.62	44.33	6.75	41.19	5.58
J2K	0.2	31.48 db	8.04	71.68	11.06	60.25	12.86	57.79	31.9 db	10.36	63.50	7.01	77.01	19.78	34.67
J2K	0.3	35.18 db	3.32	87.27	15	77.14	8.01	77.01	34.52 db	3.58	89.22	1.10	96.75	14.26	56.36
J2K	0.4	36.70 db	0.70	97.92	7.50	77.14	6.85	79.61	35.14 db	3.63	87.14	0.96	96.36	9.17	71.68
J2K	0.5	37.41 db	1.7	94.41	2.16	91.55	1.72	76.36	35.32 db	3.48	89.61	2.2	93.11	7.87	75.32
J2K	0.6	37.93 db	1.82	92.97	3.22	88.31	5.22	85.84	35.38 db	2.22	92.33	0.19	98.70	7.68	74.54
J2K	0.7	38.27 db	0.61	97.66	4.37	87.14	3.05	91.94	35.40 db	1.69	94.80	1.55	95.32	6.78	77.92
J2K	0.8	38.55 db	1.71	92.20	1.79	94.93	5.84	85.45	35.41 db	2.77	93.11	0.70	98.44	6.71	77.92
J2K	0.9	38.78 db	0.19	99.09	2.31	92.59	2.63	91.94	35.40 db	4.31	86.49	1.58	95.71	6.70	78.70
J2K	1.0	38.96 db	0.78	96.23	2.64	92.07	4.75	88.31	35.36 db	2.88	92.85	0.67	98.70	6.53	79.99
JPG	0.1	26.08 db	25.42	24.93	22.34	31.81	23.58	34.54	26.34 db	24.48	30.64	26.19	17.79	26.66	27.01
JPG	0.2	28.61 db	15.78	41.68	19.37	38.18	15.67	51.68	28.85 db	19.24	40.12	15.01	44.15	21.23	35.71
JPG	0.3	33.34 db	2.83	88.31	6.83	76.75	6.52	80.64	33.15 db	5.34	82.33	2.05	91.42	12.55	57.53
JPG	0.4	35.34 db	2.49	94.15	4.12	86.62	5.71	82.98	34.53 db	5.26	82.98	1.76	95.84	11.77	66.23
JPG	0.5	36.44 db	1.34	95.97	3.43	90.12	4.29	88.44	35.05 db	3.92	90	1.21	97.01	7.59	74.41
JPG	0.6	37.12 db	1.22	96.36	4.89	86.36	4.16	89.74	35.27 db	4.29	88.57	0.49	98.96	11.65	65.84
JPG	0.7	38.27 db	1	97.14	3.76	88.96	5.21	86.49	35.37 db	4.70	87.40	1.27	96.88	7.04	75.84
JPG	0.8	37.95 db	1.42	95.84	4.10	88.57	3.26	91.55	35.41 db	2.67	91.29	0.47	99.22	11.40	66.23
JPG	0.9	38.23 db	0.20	99.48	2.99	90.25	3.37	90.64	35.42 db	3.85	86.62	0.33	98.96	9.2	72.98
JPG	1.0	38.45 db	2.22	94.15	2.17	93.63	5.63	86.88	35.42 db	4.41	87.92	2.44	93.89	6.88	79.35
JXR	0.1	20.37 db	45.68	7.01	48.37	4.28	48.34	5.84	20.51 db	41.76	6.49	47.59	5.19	46.63	5.71
JXR	0.2	30.88 db	10.19	57.27	14.57	49.61	13.25	59.35	31.64 db	11.83	60.90	7.04	74.93	19.29	38.05
JXR	0.3	33.37 db	5.76	80.90	7.89	74.93	6.79	79.09	33.79 db	4.98	82.59	2.59	94.41	12.80	56.49
JXR	0.4	34.80 db	3.02	88.44	4.93	85.71	4.29	84.54	34.74 db	5.08	82.98	1.55	95.58	10.77	67.92
JXR	0.5	35.85 db	3.21	86.10	4.83	84.67	5.58	82.07	35.24 db	4.95	86.49	2.07	93.63	10.01	67.53
JXR	0.6	36.61 db	3.01	90.51	4.69	84.80	4.91	85.58	35.48 db	3.25	88.57	0.5	98.18	6.72	75.45
JXR	0.7	37.18 db	1.94	94.93	1.86	94.15	5.72	83.76	35.60 db	3.03	92.33	1.94	94.41	8.10	75.06
JXR	0.8	37.62 db	1.79	91.68	3.94	86.62	4.23	86.88	35.63 db	4.17	85.32	0.97	98.18	11.78	68.05
JXR	0.9	37.97 db	0.99	95.32	3.06	90.38	2.65	90.90	35.63 db	2.92	90.38	0.77	97.27	7.05	78.05
JXR	1.0	38.28 db	0.86	96.49	5.01	86.36	5.25	84.80	35.61 db	3.23	90.90	0.87	97.14	6.62	79.87

6 Discussion

While for the human eye, lossless images look superior to lossy images, we can assume that lossless image compression formats will lead to a better detection and recognition performance because of the missing block artifacts generated by the lossy JPEG image format. Contrary to this expectation, the impact of improvement through most common lossless compression formats are more in the visual domain and not affecting state-of-the-art segmentation and ear recognition classifiers. Fig. 4 show the edge compressing results for all 3 image formats with high compression ratio. We can assume, that JPEG2000 is washing out the clean edge and makes it softer like a Gaussian blur. JPEG and JPEG-XR has a bigger difference between bright and dark regions while JPG-XR compared to JPEG has more layers on the edge with decreasing brightness and adds more random pixels in the neighborhood.

7 Conclusion

In summary, ISO specification ISO/IEC 19794 [14] for biometric data interchange formats makes reference to a standard image format for biometric data for several biometrics and provides JPEG2000 as standard format for storing different biometric images except ear images. Our Results show, that better visual image quality isn't a eligible predicate in terms of segmentation and recognition accuracy. Contrary to the ISO specification where JPEG2000 is the algorithm of choice, experiments show, that lossless compression formats f.e., JPEG2000 and JPEG-XR aren't well suited compression algorithms on automated ear biometrics compared to lossy JPEG compression. In our work, JPEG delivers the best performance for automated recognition as well as for automated segmentation the outer ear. The improvements with JPEG2000 ring artifacts, affect only the visual representation for human eyes as well as wavelet based JPEG-XR but not for state-of-the-art classifiers used in this work. Ring artifacts destroy the clean edge produced by block artifacts and leads in problems for edge detecting classifiers as well as for gradient based classifiers due to washed out edges which lets us conclude, that JPEG is a more usable algorithm for ear biometrics. In future Work, we will focus on compressed classifier training set's to improve accuracy on ear recognition as well as ear detection.

References

[1] P. Erdős, *A selection of problems and results in combinatorics*, Recent trends in combinatorics (Matrahaza, 1995), Cambridge Univ. Press, Cambridge, 2001, pp. 1–6.

[2] ISO. ISO/IEC JTC1/SC 37 Standing Document 11 (SD 11), Part 1 Harmonization Document, 2010.

[3] A. Abaza and M. A. F. Harrison, *Ear recognition: a complete system*, SPIE 8712, Biometric and Surveil- lance Technology for Human and Activity Identification, 2013.

[4] Anil K. Jain, et. al, *An Introduction to Biometric Recognition*, 4 IEEE Transactions On Circuits And Systems For Video Technology, vol. 14, No. 1, 2004.

[5] Anika Pflug, Christoph Busch, *Ear Biometrics: A Survey of Detection, Feature Extraction and Recognition Methods*, IET Biometrics, 2012.

[6] David J. Hurley, *Force Field Feature Extraction for Ear Biometrics*, UNIVERSITY OF SOUTHAMPTON, PhD Thesis, September 2001.

[7] Papageorgiou, Oren and Poggio, *A general framework for object detection*, International Conference on Computer Vision, 1998

[8] A. Bertillon, *La Photographie Judiciaire: Avec Un Appendice Sur La Classification Et LâIdentification An- thropometriques*, Gauthier-Villars, Paris, 1890

[9] A.V.Iannarelli,*Earidentification*,ParamontPublishing Company, 1989.

[10] Wikipedia, *Histogram of oriented gradients*,`https://en.wikipedia.org/wiki/Histogram_of_oriented_gradients`, March,5th 2014

[11] Rahtu E., Ojansivu V. , Heikkila J. ,*Recognition of blurred faces using Local Phase Quantization*, 19th International Conference on Pattern Recognition, 2008.

[12] University of Oulu, *Local Binary Pattern*, `http://www.cse.oulu.fi/CMV/Research/LBP`,March,5th 2014

[13] Stan Z. Li, et. al, *Encyclopedia of Biometrics*, Springer US, 2009.

[14] International Standard ISO/IEC 19794, *Information technology – Biometric data interchange formats –*

[15] Paul Viola and Michael Jones, *Robust real-time object detection* International Journal of Computer Vision, 2002.

[16] ISO/IEC 15444-14:2013 *JPEG 2000 image coding system*

[17] ISO/IEC 10918-1:1994 *Information technology – Digital compression and coding of continuous-tone still images, lossless*.

[18] ISO/IEC 29199-2:2010 *Information technology – JPEG XR image coding system.*

[19] C. Sforza And G. Grandi And M. Binelli And D. G. Tommasi And R. Rosati And V. F. Ferrario, *Age- and sex-related changes in the normal human ear*, Forensic Science International, 2009.

[20] Johannes Wagner, Anika Pflug, Christian Rathgeb, Christoph Busch, *Effects of Severe Signal Degradation on Ear Detection*, In Proceedings of the 2nd International Workshop on Biometrics and Forensics, 2014.

[21] T. C. Faltemier, K. W. Bowyer, and P. J. Flynn, *Rotated Profile Signatures for robust 3D Feature Detection", in Automatic Face and Gesture Recognition*, 2008.

[22] P. Yan and K. W. Bowyer, *Biometric Recognition Us- ing 3D Ear Shape*, Pattern Analysis and Machine Intel- ligence, vol. 29, pp. 1297 â 1308, 2007.

[23] P. Yan and K. W. Bowyer, *An Automatic 3D Ear Recognition System*, in 3rd Symposium on 3D Data Processing, Visualization, and Transmission, 2006.

[24] Navneet Dalal, *Finding People in Images and Videos*, P.hD. Thesis, 2006

8 Appendix

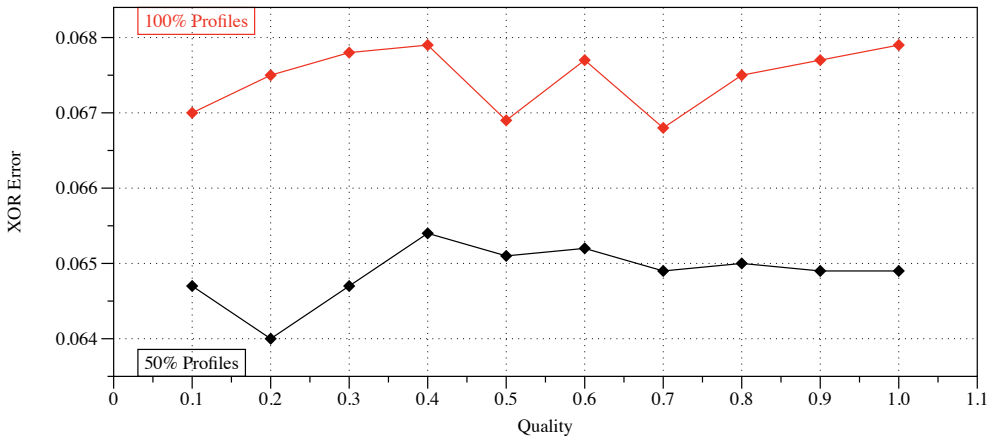

Figure 15: Detection Error for Haar-like features in combination with JPEG2000 compression

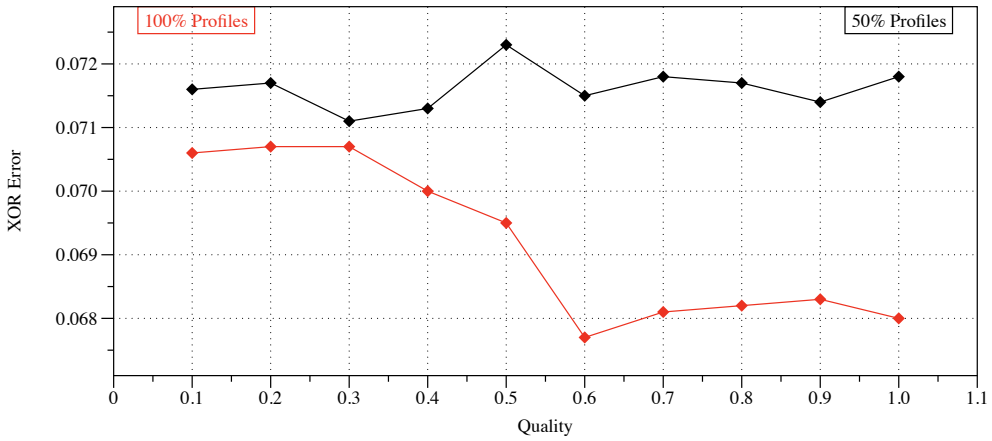

Figure 16: Detection Error for HOG features in combination with JPEG2000 compression

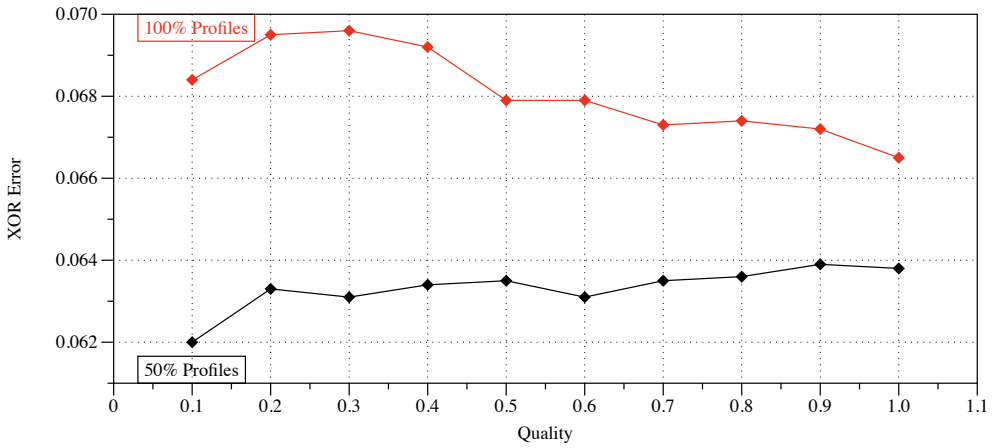

Figure 17: Detection Error for LBP features in combination with JPEG2000 compression

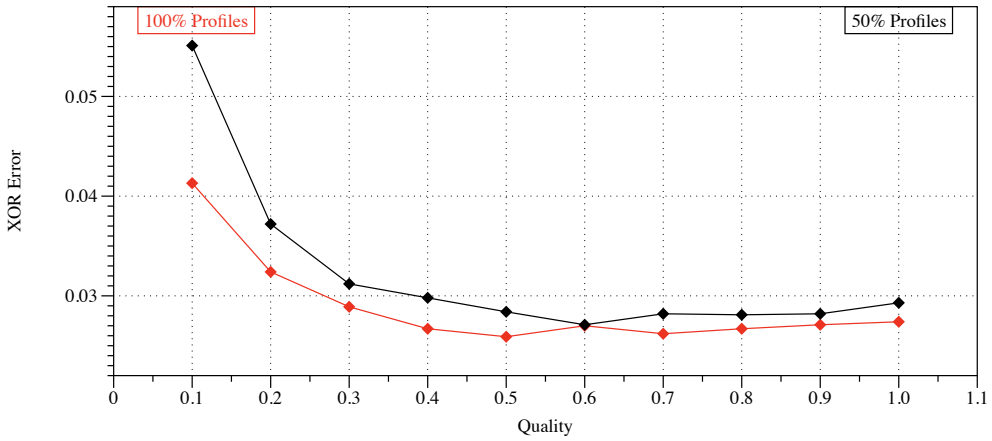

Figure 18: Detection Error for Haar-like features in combination with JPEG compression

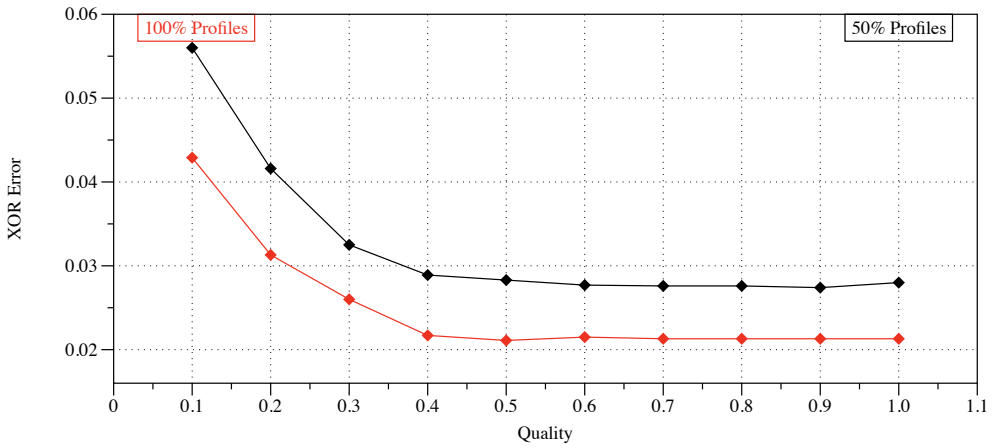

Figure 19: Detection Error for HOG features in combination with JPEG compression

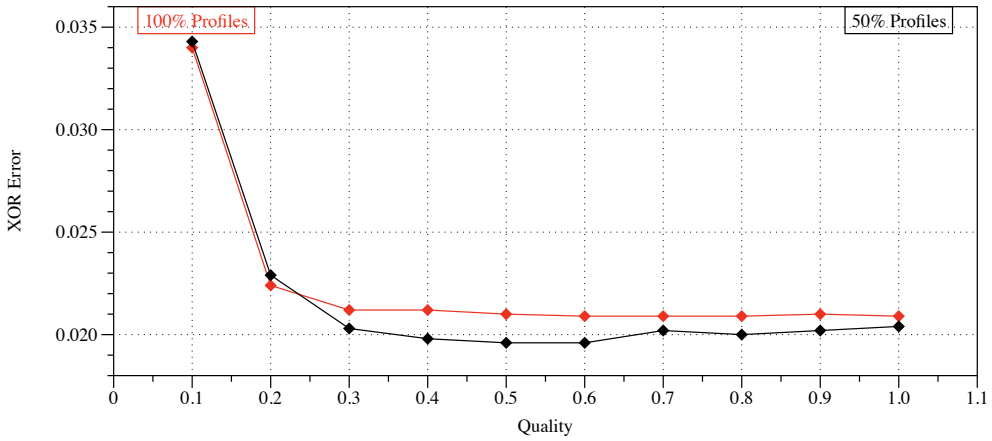

Figure 20: Detection Error for LBP features in combination with JPEG compression

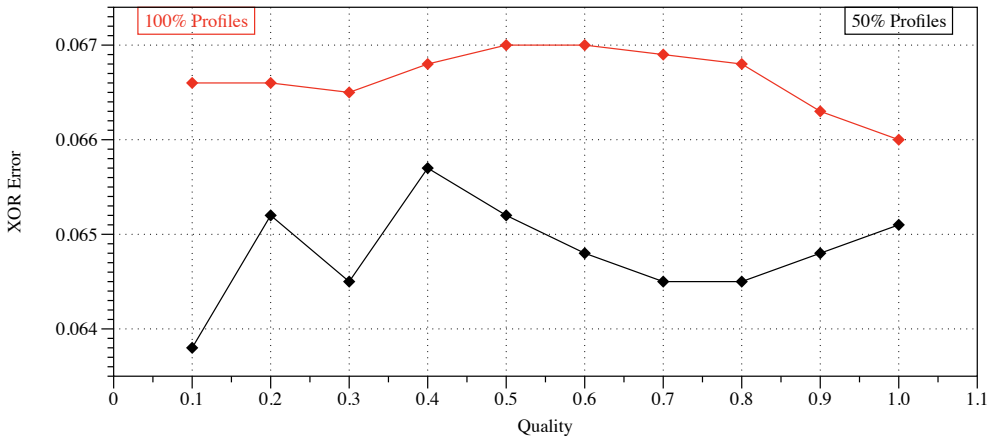

Figure 21: Detection Error for Haar-like features in combination with JPEG-XR compression

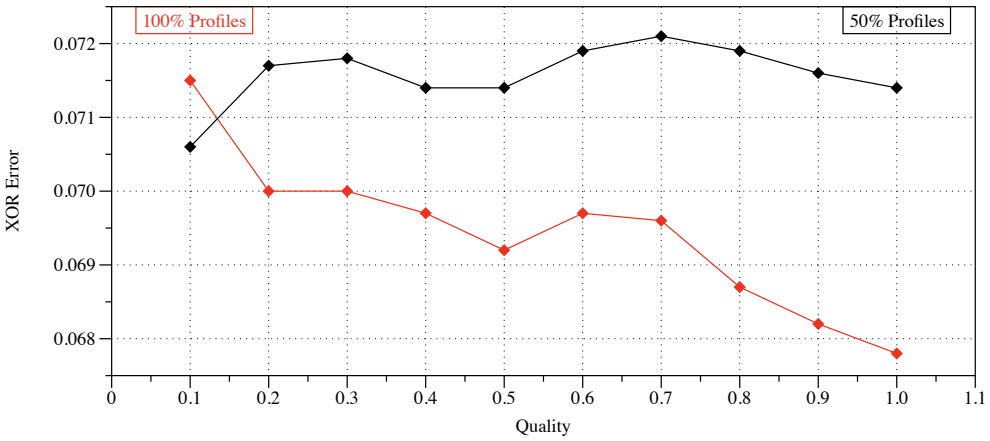

Figure 22: Detection Error for HOG features in combination with JPEG-XR compression

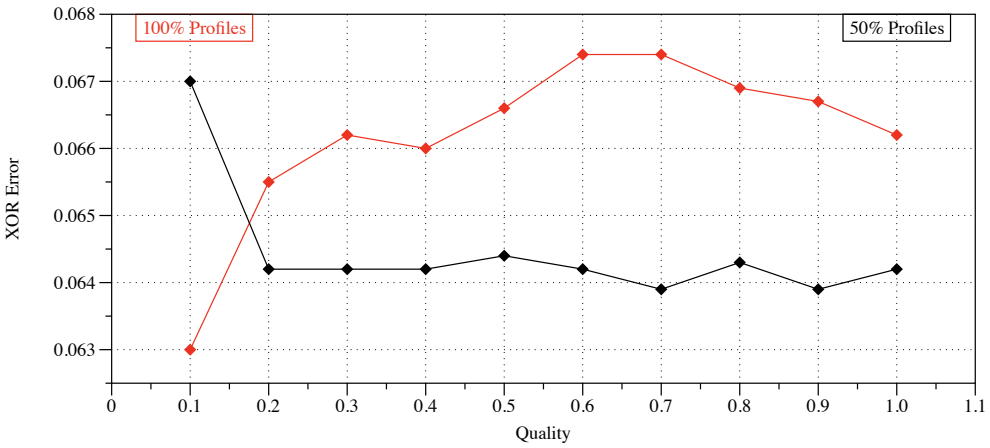

Figure 23: Detection Error for LBP features in combination with JPEG-XR compression

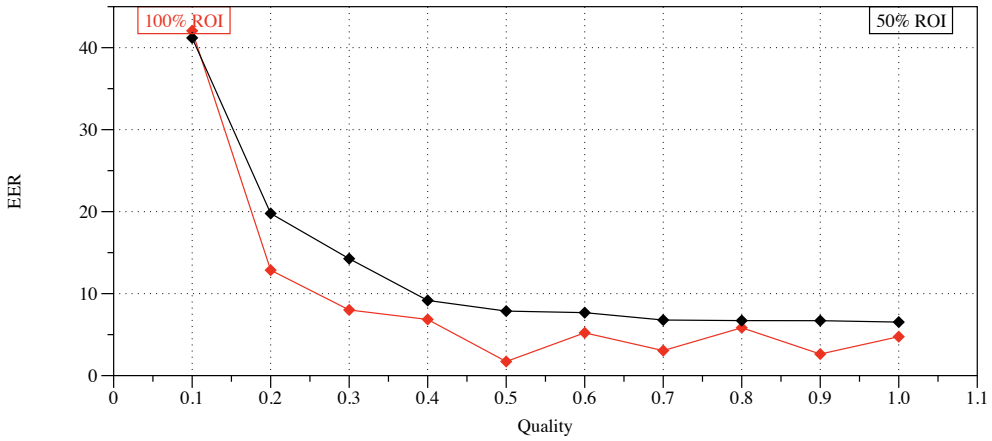

Figure 24: Equal Error Rates for HOG features on JPEG2000 with different compression rates

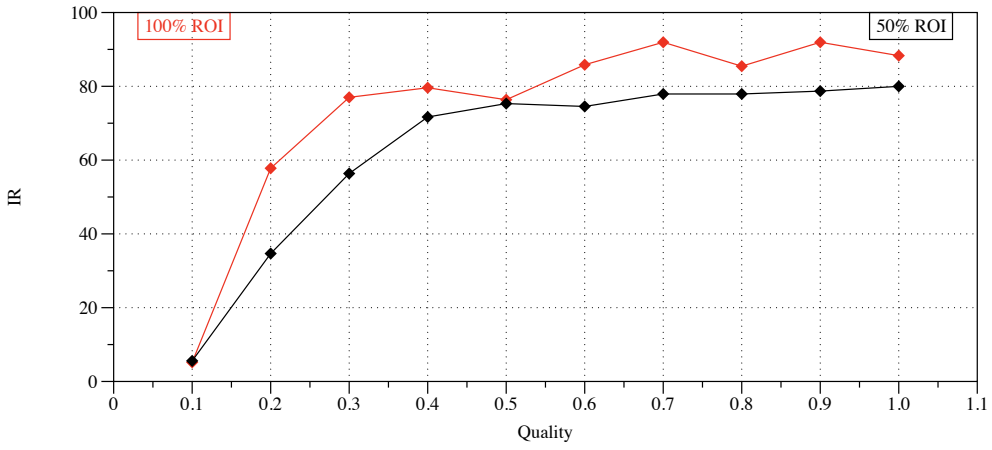

Figure 25: Identification Rates for HOG features on JPEG2000 with different compression rates

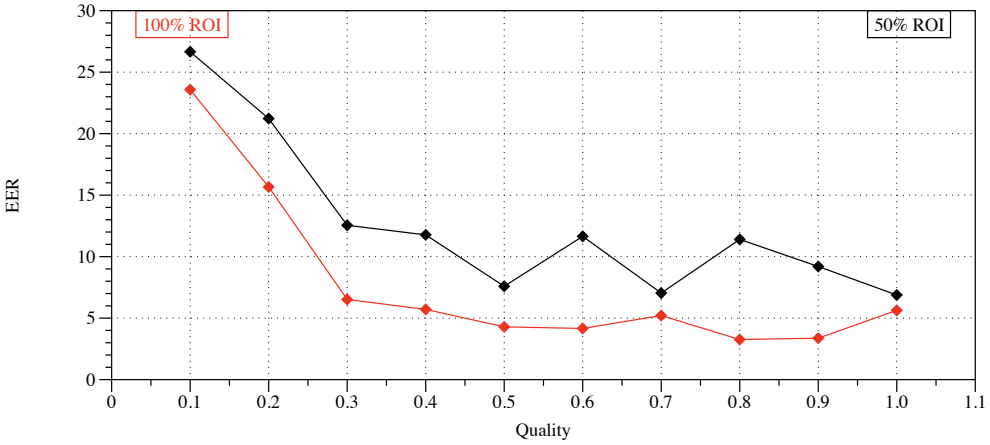

Figure 26: Equal Error Rates for HOG features on JPEG with different compression rates

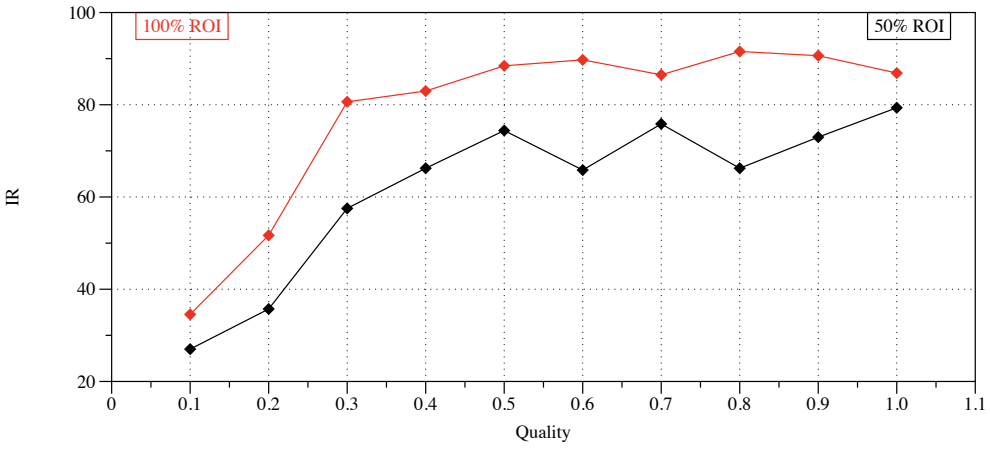

Figure 27: Identification Rates for HOG features on JPEG with different compression rates

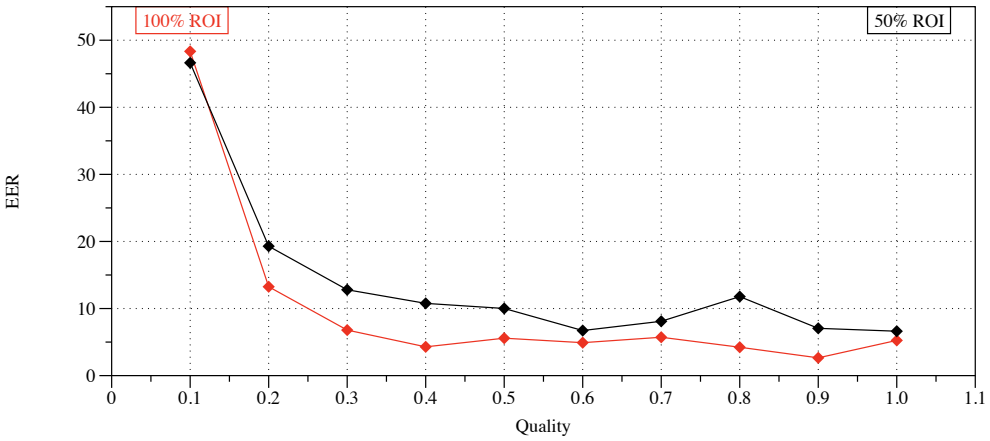

Figure 28: Equal Error Rates for HOG features on JPEG2000 with different compression rates

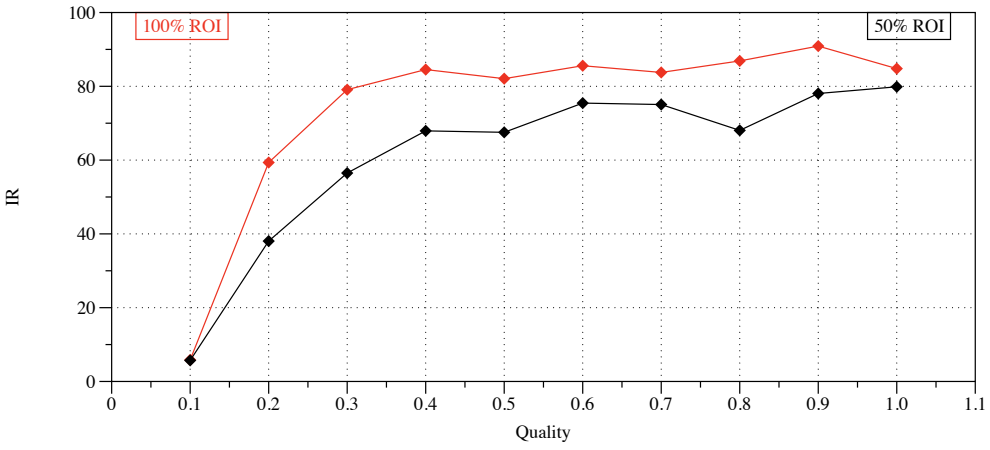

Figure 29: Identification Rates for HOG features on JPEG2000 with different compression rates

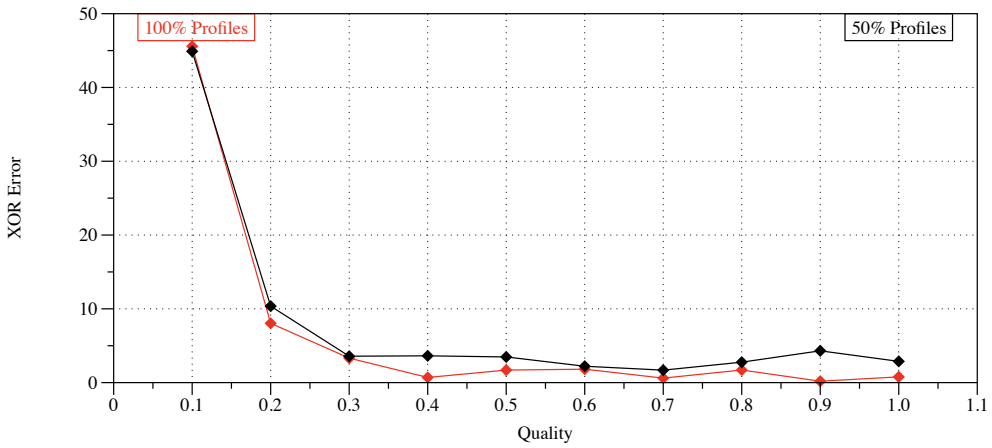

Figure 30: Equal Error Rates for LBP features on JPEG2000 with different compression rates

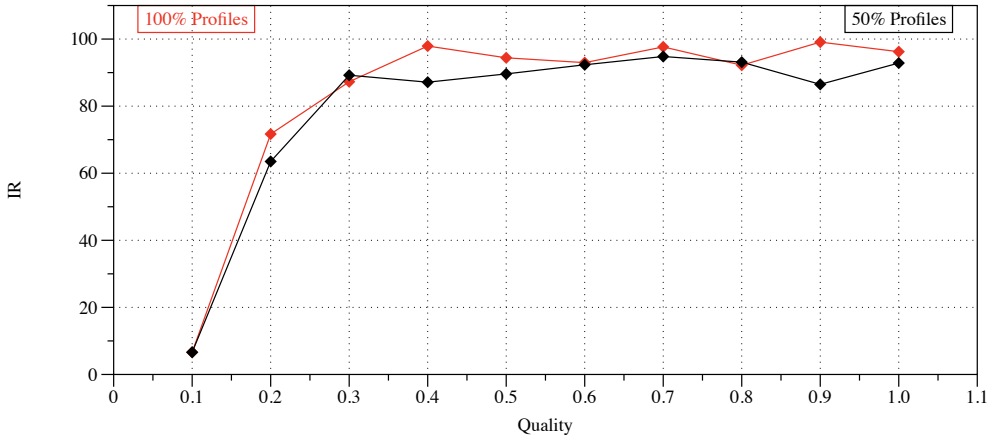

Figure 31: Identification Rates for LBP features on JPEG2000 with different compression rates

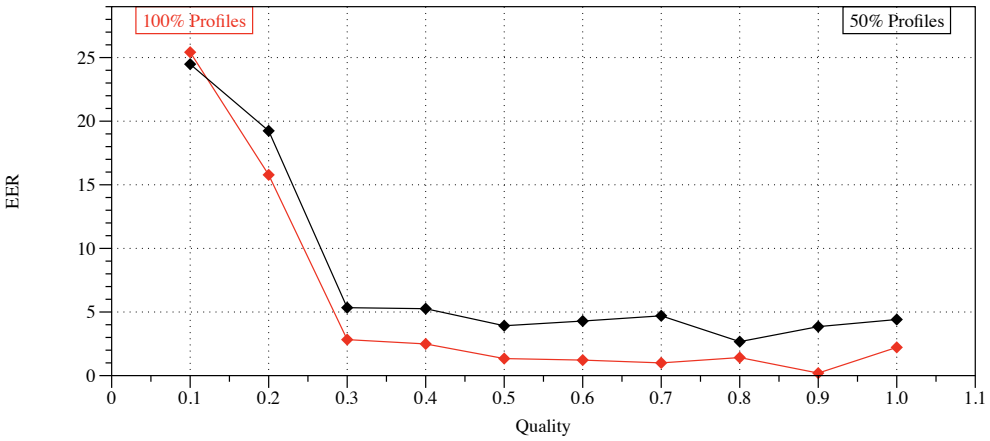

Figure 32: Equal Error Rates for LBP features on JPEG with different compression rates

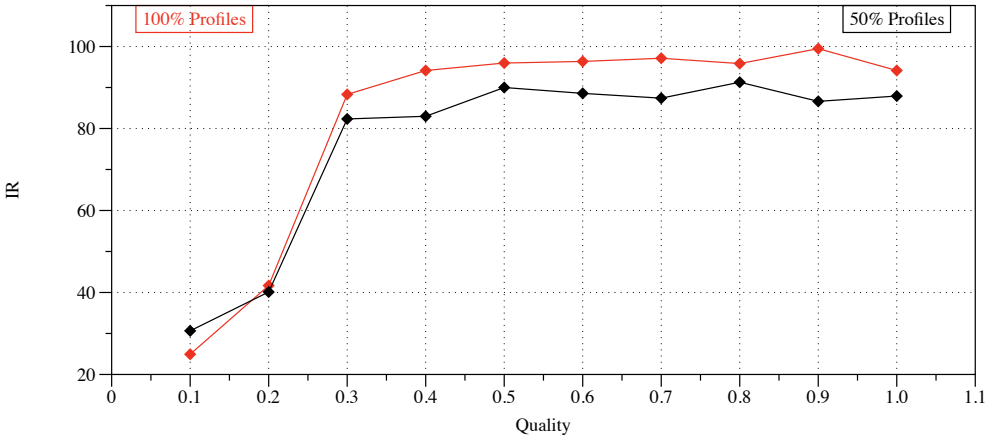

Figure 33: Identification Rates for LBP features on JPEG with different compression rates

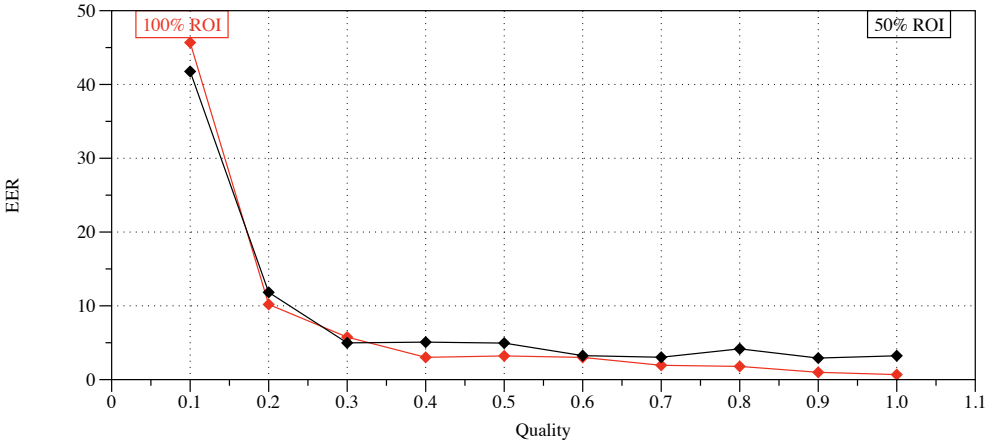

Figure 34: Equal Error Rates for LBP features on JPEG2000 with different compression rates

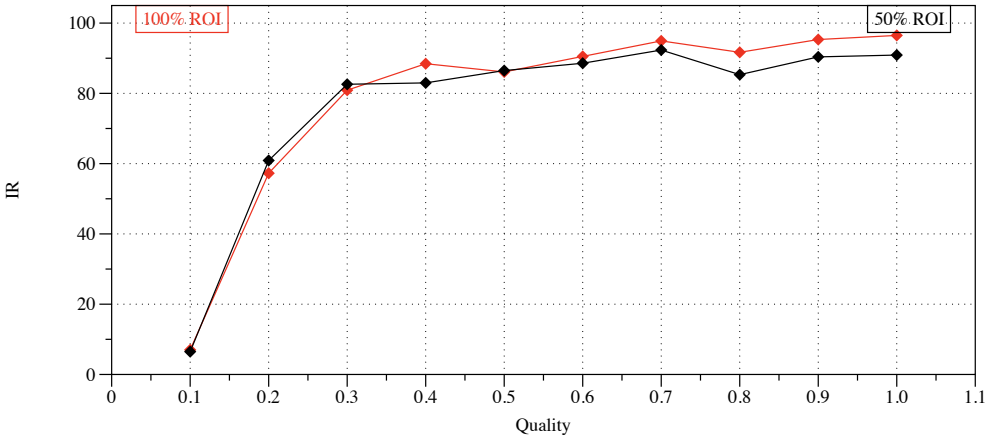

Figure 35: Identification Rates for LBP features on JPEG2000 with different compression rates

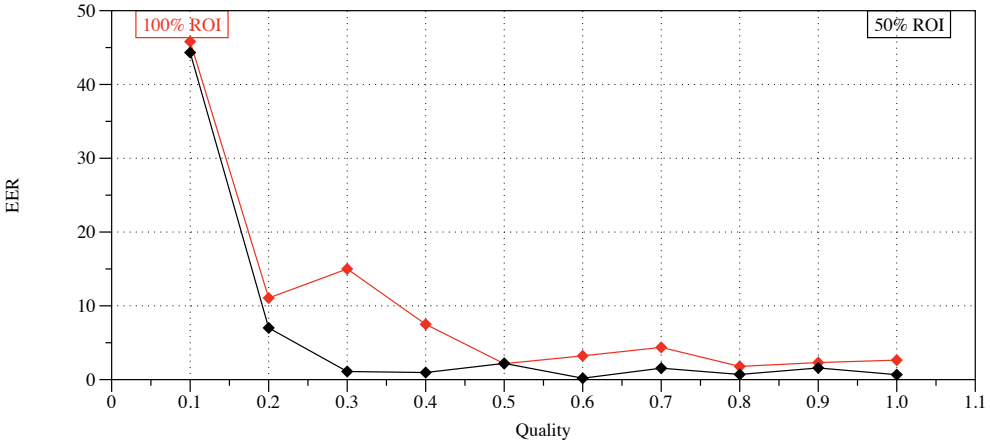

Figure 36: Equal Error Rates for LPQ features on JPEG2000 with different compression rates

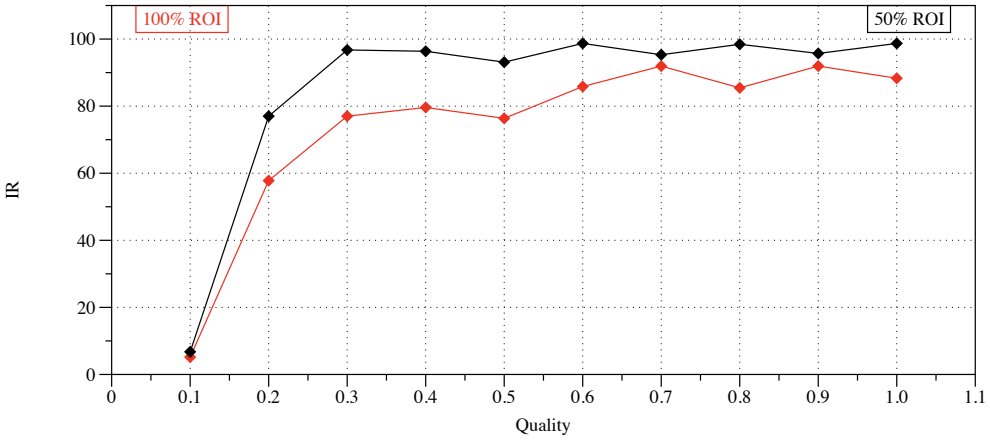

Figure 37: Identification Rates for LPQ features on JPEG2000 with different compression rates

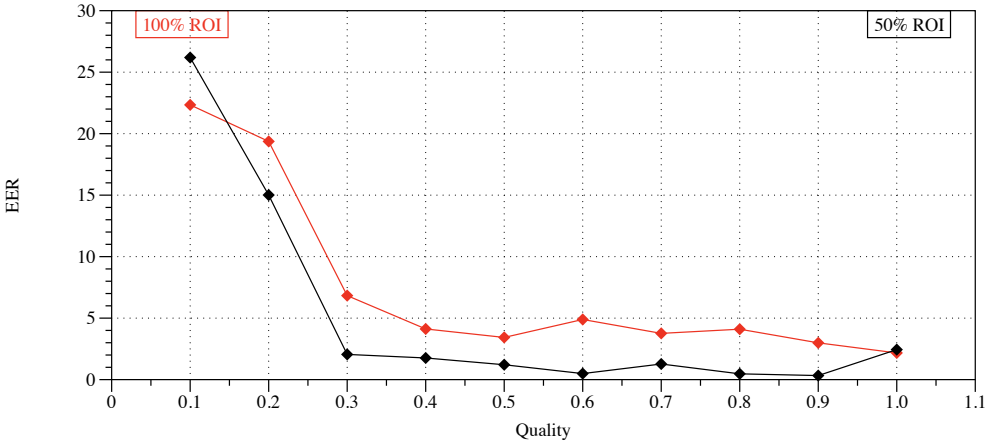

Figure 38: Equal Error Rates for LPQ features on JPEG with different compression rates

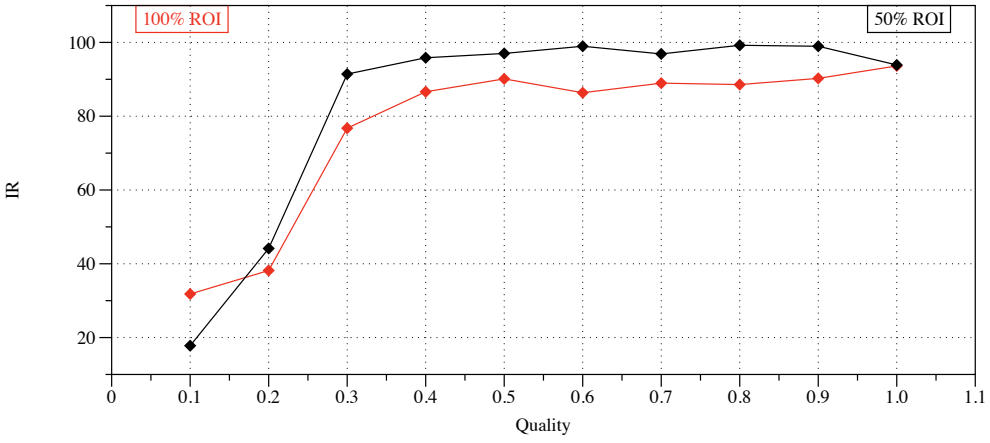

Figure 39: Identification Rates for LPQ features on JPEG with different compression rates

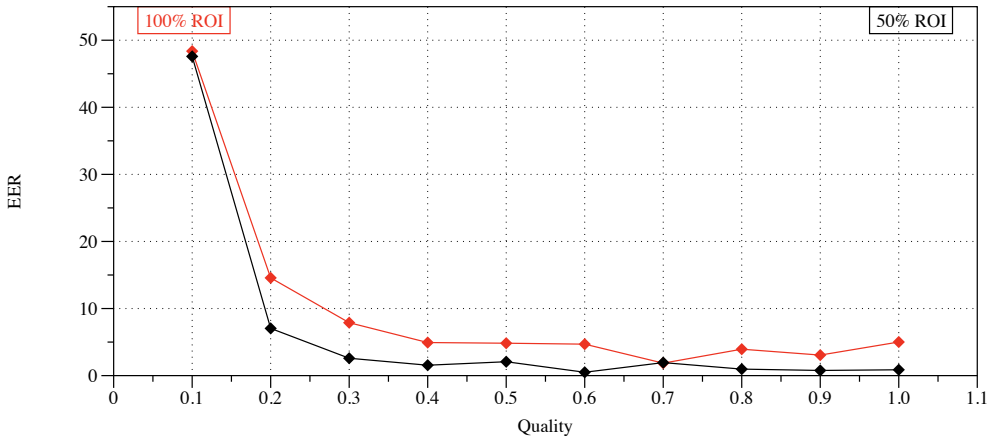

Figure 40: Equal Error Rates for LPQ features on JPEG2000 with different compression rates

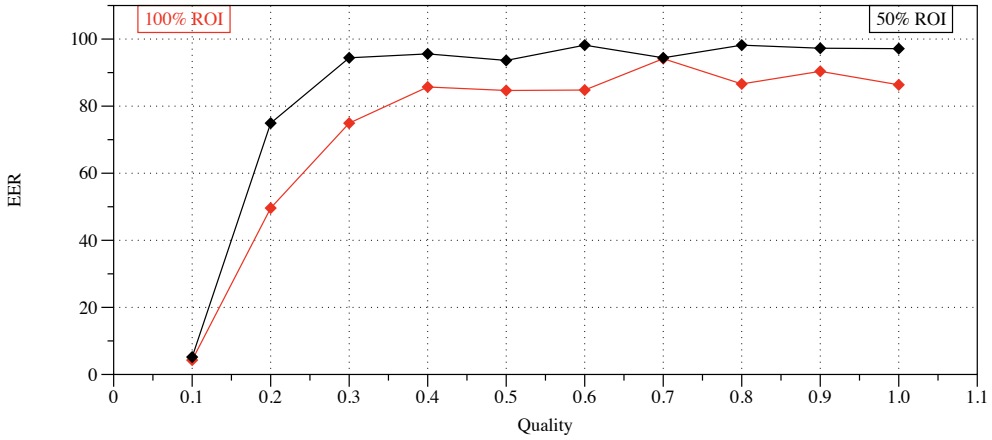

Figure 41: Identification Rates for LPQ features on JPEG2000 with different compression rates

Table 5: JPEG2000 compressing stages 0.1 – 1.0 shown on full profile sample image.

(a) 0.1 bpp

(b) 0.2 bpp

(a) 0.3 bpp

(b) 0.4 bpp

(a) 0.5 bpp

(b) 0.6 bpp

(a) 0.7 bpp

(b) 0.8 bpp

(a) 0.9 bpp

(b) 1.0 bpp

Table 6: JPEG compressing stages 0.1 – 1.0 shown on full profile sample image.

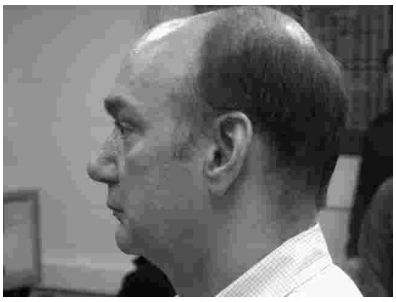

(a) 0.1 bpp

(b) 0.2 bpp

(a) 0.3 bpp

(b) 0.4 bpp

(a) 0.5 bpp

(b) 0.6 bpp

(a) 0.7 bpp

(b) 0.8 bpp

(a) 0.9 bpp

(b) 1.0 bpp

Table 7: JPEG-XR compressing stages 0.1 – 1.0 shown on sample image.

(a) 0.1 bpp

(b) 0.2 bpp

(a) 0.3 bpp

(b) 0.4 bpp

(a) 0.5 bpp

(b) 0.6 bpp

(a) 0.7 bpp

(b) 0.8 bpp

(a) 0.9 bpp

(b) 1.0 bpp

Table 8: JPEG2000 compressing stages 0.1 – 1.0 shown on 100×100 ROI sample image.

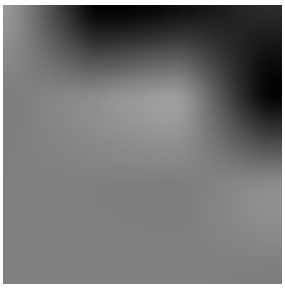

(a) 0.1 bpp

(b) 0.2 bpp

(a) 0.3 bpp

(b) 0.4 bpp

(a) 0.5 bpp

(b) 0.6 bpp

(a) 0.7 bpp

(b) 0.8 bpp

(a) 0.9 bpp

(b) 1.0 bpp

Table 9: JPEG compressing stages 0.1 – 1.0 shown on 100×100 ROI sample image.

(a) 0.1 bpp

(b) 0.2 bpp

(a) 0.3 bpp

(b) 0.4 bpp

(a) 0.5 bpp

(b) 0.6 bpp

(a) 0.7 bpp

(b) 0.8 bpp

(a) 0.9 bpp

(b) 1.0 bpp

Table 10: JPEG-XR compressing stages 0.1 – 1.0 shown on 100×100 ROI sample image.

(a) 0.1 bpp

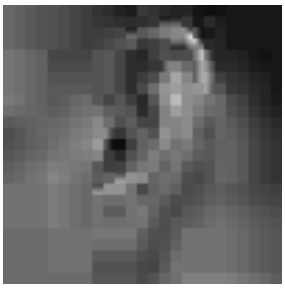

(b) 0.2 bpp

(a) 0.3 bpp

(b) 0.4 bpp

(a) 0.5 bpp

(b) 0.6 bpp

(a) 0.7 bpp

(b) 0.8 bpp

(a) 0.9 bpp

(b) 1.0 bpp